國立臺灣大學電機資訊學院電信工程學研究所
碩士論文
Graduate Institute of Communication Engineering
College of Electrical Engineering and Computer Science
National Taiwan University
Master Thesis

IEEE 802.11ax 基於OFDMA隨機接取效能分析
Performance Analysis of IEEE 802.11ax OFDMA-based Random Access

楊行
Yang Hang

指導教授：陳光禎 博士
Advisor: Kwang-Cheng Chen, Ph.D.

中華民國 105 年 12 月
December, 2016

doi:10.6342/NTU201700509

致謝

黑夜給了我黑色的眼睛
我卻用它尋找光明

顧城,1979

doi:10.6342/NTU201700509

中文摘要

下一代無線區域網路802.11ax面對密集場景對接取層（MAC），物理層（PHY）層都做出巨大修改。它提出一個基於OFDMA的多通道隨機接取機制。 該論文通過拓展Bianchi的二維馬爾科夫鏈模型完成對這個基於正交頻分多址(OFDMA)的隨機接取機制的穩態的行爲進行預測，預測是在飽和數據量的條件下進行的。 模擬的結果也驗證了該馬爾科夫鏈模型的準確性。最終，我們也分析了關鍵系統參數的影響，包括多通道的數量，初始競爭窗口以及最大競爭窗口大小。

關鍵詞： 多信道Aloha, 隨機接取, 碰撞解決, 正交頻分多址, 802.11ax.

doi:10.6342/NTU201700509

Abstract

Confronting the dense scenario, 802.11ax, the next generation WLAN, makes revolutionary modifications on both MAC and PHY layers, exploiting MU-OFDMA PHY and centralized MAC scheme. A multi-channel random access mechanism, OFDMA-based random access (OBRA) is proposed. This work extends Bianchi's bi-dimension Markov chain model to depict the steady-state behavior of the OBRA under saturation condition. And simulations validate the accuracy of the Markov chain model. Finally, the effects of system parameters, including the number of resource units (RUs) for random access, initial and maximum contention window, are evaluated.

Keywords: multi-channel slotted Aloha, random access, collision resolution, OFDMA, 802.11ax.

doi:10.6342/NTU201700509

Contents

口試委員會審定書 **i**

致謝 **ii**

中文摘要 **iii**

Abstract **iv**

1 Introduction **1**

1.1 Background 1

1.2 Challenge of WiFi 4

1.3 Solution: 802.11ax 8

1.4 Related Works 9

1.5 Motivation 11

1.6 Organization 11

2 802.11ax Features **12**

2.1 MU-OFDMA 12

2.2 802.11ax Random Access Illustration 14

3 System Model **17**

3.1 Packet Transmission Probability 18

3.2 Random Access Efficiency 23

3.2.1 n_s and System Efficiency 24

3.2.2 Access Delay 24

doi:10.6342/NTU201700509

3.3 Model Validation 25

4 Performance Evaluation **27**

4.1 Maximum System Efficiency and Minimum Access Delay 27

4.2 Effects of System Parameter 29

4.2.1 RUs for Random Access M 30

4.2.2 Initial and max Contention Window (OCW_{min}, OCW_{max}) 30

4.2.3 Rules for configuring $\{M, OCW_{min}, OCW_{max}\}$ 32

5 Conclusion and Future work **38**

Bibliography **39**

doi:10.6342/NTU201700509

List of Figures

1.1 Working mode of WiFi 2
1.2 DCF working procedure 4
1.3 Saturated analysis: throughput vs number of stations 6
1.4 Partition of working states of a station under saturated condition 7
1.5 Energy consumption of a station under saturated condition 7
1.6 Unfair queueing problem of BSS 8

2.1 MU DL of 802.11ax 13
2.2 Trigger-based MU UL of 802.11ax 13
2.3 Trigger Frame format 14
2.4 An example of Trigger-based MU UL transmission with OBRA 15
2.5 Illustration of OBRA 15
2.6 Random Access Parameter Set (RAPS) Element 16

3.1 Concept of time in OFDMA-based random access 18
3.2 Markov Chain model for the backoff window size 20
3.3 System efficiency: Analysis versus Simulation 26

4.1 Efficiency and access delay versus transmission probability τ 28
4.2 Configure M 33
4.3 Transmission probability τ versus number of stations 34
4.4 Details of transmission probability τ versus number of stations when $n \leq 100$ 35
4.5 Example of Configuring OCW_{max}, given $M = 9$ 36

doi:10.6342/NTU201700509

4.6 Example of Configuring OCW_{min}, given $M = 18$ 37

doi:10.6342/NTU201700509

List of Tables

1.1 Overview of 802.11 PHYs 3

2.1 Maximum number of RUs for each channel width 13

3.1 Parameters and Notations Interpretation 18

3.2 Analysis versus simulation: n_s and access delay with $m = 3, M = 9, OCW_{min} = 15$ 26

doi:10.6342/NTU201700509

Chapter 1

Introduction

1.1 Background

IEEE 802.11

Wireless local area networking (WLAN) has experienced tremendous growth in the last two decades for its high throughput and simplicity of implementation. WLAN liberates people from fixed cable so that they could access to the world anywhere and anytime. IEEE 802.11 standardizes one type of WLAN on ISM band, which is free for commercial use from 1985. The first version of the 802.11 standard was ratified in 1997. As a member of the IEEE 802.11 family of local area networking (LAN) and metropolitan area networking (MAN) standards, 802.11 interfaces with 802.1 architecture, management, and interworking, and 802.1 logical link control (LLC). The combination of 802.2 LLC and 802.11 MAC and PHY make up the data link and physical layers of the Open Systems Interconnection (OSI) reference model[2]. The IEEE 802.11 working group began development of a common medium access control (MAC) layer for multiple physical layers (PHY) to standardize WLAN [3]. To interoperate between IEEE 802.11 devices from different manufacturers, the Wi-Fi Alliance (WFA)[4] was formed in 1999 to certify interoperability by rigorous testing.

802.11 WLAN has two working modes, infrastructure basic service set (BSS) and independent BSS, see Fig. 1.1. The infrastructure BSS consists of one access point (AP)

doi:10.6342/NTU201700509

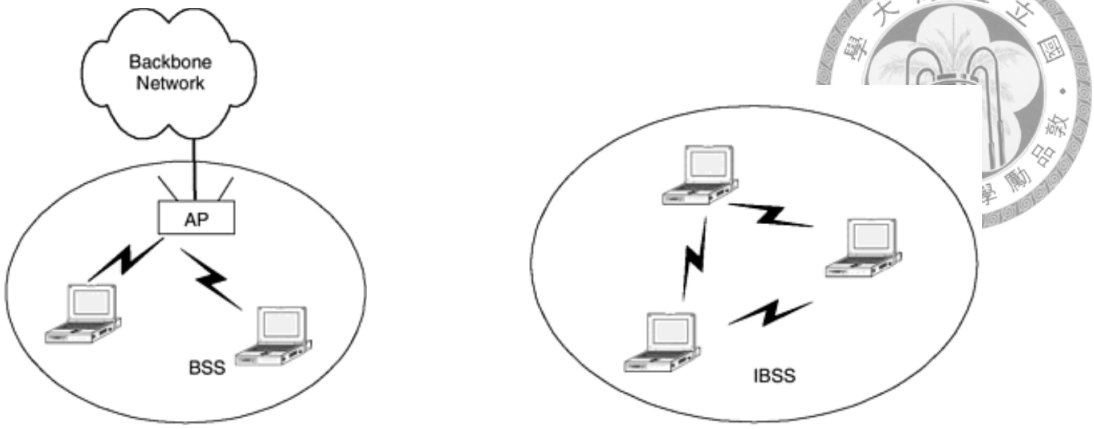

(a) Infrastructure mode (b) Ad hoc mode

Figure 1.1: Working mode of WiFi

and multiple stations (STA) as Fig. 1.1a, forming a star topology. That means stations could only communicate with AP instead of communicate with each other directly. And we call the direction from AP to stations down-link (DL) and from stations to AP up-link (UL). The other mode is Independent BSS (IBSS), also called ad-hoc network, see Fig. 1.1b. In the IBSS, all stations are equal and could communicate with each other directly only if the two stations could detect each other. In this thesis, only the infrastructure mode is considered.

The original 802.11 standard (1997) included three PHYs: infrared (IR), 2.4 GHz frequency hopped spread spectrum (FHSS), and 2.4 GHz direct requence spread spectrum (DSSS). The DSSS supports data rates of 1, 2 Mbps on a 20 MHz channel. This was followed by two standard amendments in 1999: 802.11b built upon enhanced DSSS with complementary code keying (CCK) to increase data rate to 11 Mbps at 2.4 GHz and 802.11a to solicit OFDM PHY at 5GHz with data rate up to 54 Mbps. However, 802.11a is not accepted widely for its non-compatibility while 802.11b experiences a tremendous growth. Subsequently, the 802.11 working group developed 802.11g amendment to help maintain backward compatibility and interoperability. Afterward, 802.11n, the High Throughput (HT) Study Group, improved data rate by spatial multiplexing using Multiple-input and Multiple-output (MIMO)[5] and 40 MHz operation. A device equiped with multiple antennas may support at most 4 streams with MIMO. To take advantage of the much higher data rates provided by these techniques, MAC efficiency is also im-

doi:10.6342/NTU201700509

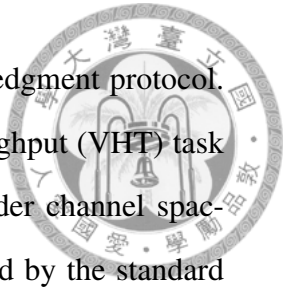

proved by frame aggregation and enhancements to the block acknowledgment protocol. Until 2013, to satisfy increasing mobile demand, the Very High Throughput (VHT) task group 802.11ac (TGac) was ratified, with even more streams and wider channel spacing. Furthermore, a multi-user (MU) PHY, MU-MIMO[6] was defined by the standard as a technique where multiple stations, each with potentially multiple antennas, transmit and/or receive independent data streams simultaneously.[7] That is, MU-MIMO allows AP having multiple antennas to transmit several data streams to multiple users at the same time over the same frequency channel. However, the MU-MIMO only supports DL transmission, namely from AP to stations.

Table 1.1: Overview of 802.11 PHYs

	802.11	802.11b	802.11g	802.11n	802.11ac
PHY technology	DSSS	DSSS-CCK	OFDM/ DSSS	MIMO-OFDM	MIMO-OFDM
Data rates	1,2 Mbps	5.5,11 Mbps	1-54 Mbps	6-600 Mbps	6-1300 Mbps
Frequency band	2.4 GHz	2.4 GHz	2.4/5 GHz	2.4/5 GHz	2.4/5 GHz
Channel spacing	20 MHz	20 MHz	20 MHz	20,40 MHz	20,40,80,160 and 80+80 MHz
Maximum streams	1	1	1	4	8

Medium Access Control of 802.11

Influenced by the huge market success of Ethernet (standarded as IEEE 802.3), the 802.11 MAC adopts a similar distributed access protocol, carrier sense multiple access (CSMA). With CSMA, a station with non-empty queueing listens to the medium for a predetermined period, called dilivery inter-frame spacing (DIFS) before it transmits a packet. If the medium is sensed to be idle during this period then the station is permitted to transmit. If the medium is sensed to be busy, the station has to defer its transmission with a random period, called backoff time. The backoff time is randomly generated among a contention window. Then the the station could not transmit until backoff counter decreases to zero. Since collision is hard to be detected by transmitter, a variant CSMA/collision avoidance

doi:10.6342/NTU201700509

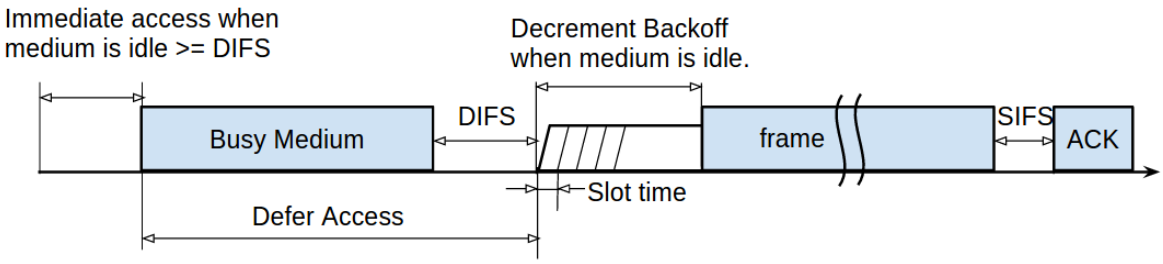

Figure 1.2: DCF working procedure

(CA) is exploited by 802.11 WLAN, therein the backoff counter could not decrease until the channel is sensed idle. Also, once a transmission fails, the contention window will be doubled, which is called binary exponential backoff (BEB). In radio network, the channel is vulnerable to interference and fading. Thus, a two-way handshake is used to determine whether the transmission is successful or not. The acknowledge frame is responded after short IFS (SIFS), equal to the duration of receiving, processing the transmitted frame and generating an ACK frame. [8]

Above all, the foundation of MAC, Distributed Coordination Function (DCF), remains during the evolution from 802.11b to 802.11ac for its robustness and simplicity. The details are all demonstrated in Fig. 1.2.

1.2 Challenge of WiFi

According to Cisco Visual Network index[9], the mobile traffic will increase 53% at CAGR within 2015-2020 reaching 30.6 EB per month by 2020, which means eight-fold increase during the 5 years. The scenarios of 802.11 WLAN are becoming more and more dense, plenty of stations in a BSS or plenty of BSSs in a limited area. The dense scenarios, according to the TGax simulation scenario [10] of 802.11ax, are various, such as enterprise building with dense deployment of BSS or indoor/outdoor hotspot with dense users etc. Interference and collisions are becoming the major obstacle to high throughput and delay performance. Evolution of legacy 802.11, 802.11 b/g/n/ac, always concentrate on improving data rate of PHY from 2 Mbps to beyond 1 Gbit/s. However, the quality of experience (QoE) [11] does not improve enough with the PHY's growth. Though previous amendments have made some improvements, especially in 802.11n, including

doi:10.6342/NTU201700509

aggregation of packets, block ACK mechanism, reduced IFS (RIFS) etc. Something defects inherent are not modified if the foundation DCF is not changed.

This section will demonstrate that DCF is not efficient under the dense scenario as a result of two causes, instability of DCF and unfair queueing problem.

Instability of DCF

Since DCF is a random access protocol, CSMA/CA could not avoid all collisions, especially in a real world with hidden terminal problem [12] and non-ideal channel. The instability means that, in some scenario, bandwidth is all consumed by collisions and no transmission is successful. The random access mechanism is inherently unstable [13], DCF is also unstable though with backoff collision resolution etc.. Actually, RTS/CTS mechanism, a four-way handshake reservation mechanism, is a good approach to mitigating collisions. However, since RTS/CTS protects data transmission with the cost of more overhead of control frame exchange, it is often not enabled only if the packet length exceeds a threshold, 2346 bytes as default.

Bianchi [14] conducts a simple and accurate bi-dimensional Markov chain model of DCF under saturation condition, which means stations are always equipped with non-empty queue. The throughput of Bianchi's work is defined as fraction of duration the channel is occupied by successfully transmitting payload. As in Fig. 1.3, the throughput degrades sharply with the number of stations increasing. We could extend Bianchi's analysis to evaluate the energy performance. Stations have roughly three working states, "transmit", "receive" and "idle". Check the Fig. 1.4, with the number of stations increasing, the partition of time in transmit state for each station decreases fast while the partition in receive state increases much, which means a station has decreasing chance to access the medium. Most of bandwidth is occupied by collisions since the throughput is decreasing. Then let's look at the energy performance by checking the Fig. 1.5. We find that total energy consumption of a station increase a lot while successful transmissions are less. Most of energy are wasted on listening to collided transmissions. DCF is not efficient under dense scenario.

doi:10.6342/NTU201700509

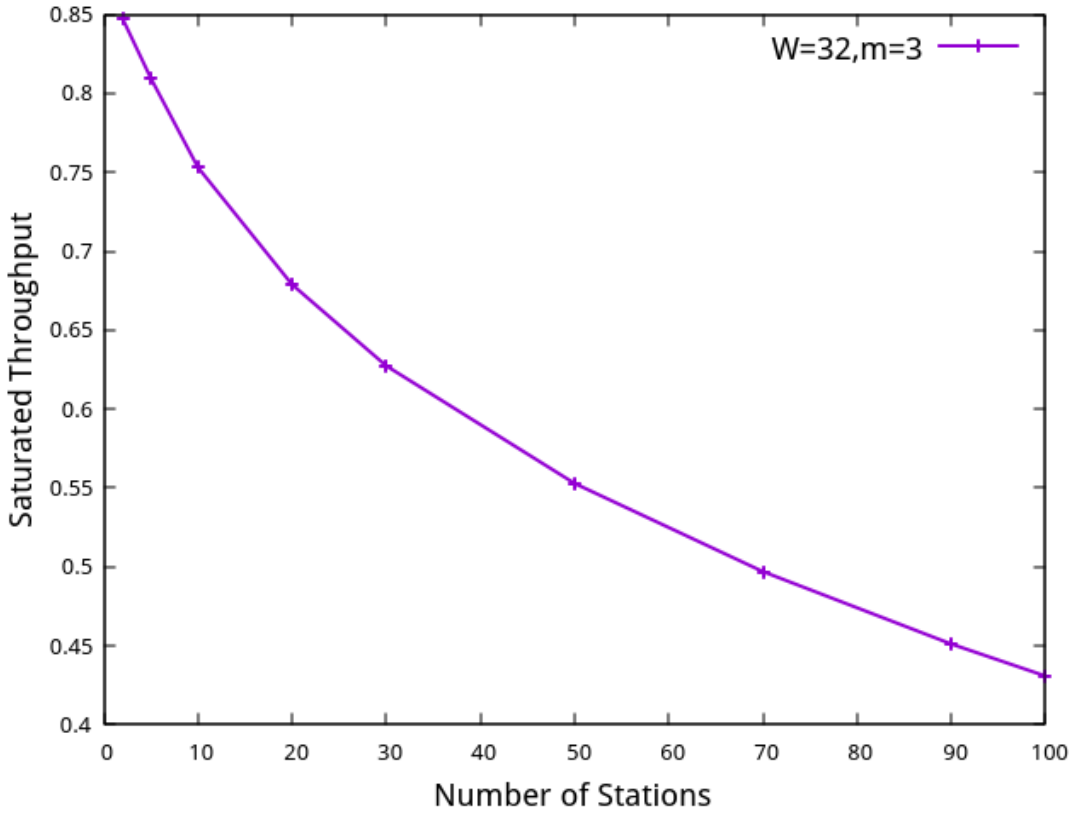

Figure 1.3: Saturated analysis: throughput vs number of stations

Unfair Queueing Problem

DCF together with the star topology of a BSS results in a absolutely unfair queueing [15]. Check the Fig. 1.6. When we see the BSS with queue model, each station, including AP, will be a queue, channel is the server. Channel capacity determines the service rate. Since BSS is star topology, access point (AP) undertakes all the down-link (DL) traffic, which is more than 1/2 traffic loading of a BSS. However, with DCF, AP has only chance of $1/(n+1)$ to access medium where n is the number of stations excluding AP. It is thus an unfair queueing for DL transmission. This problem may not degrade the performance when the "server" is fast enough. That's what a list of previous amendments, like 802.11n and ac, were doing, improving data rate of PHY from 2 Mbit/s to 7 Gbit/s. However, this solution doesn't resolve the unfair queueing inherently. The unfair queueing is always there only if the BSS with star topology is equipped with DCF. Once the BSS becomes congested

doi:10.6342/NTU201700509

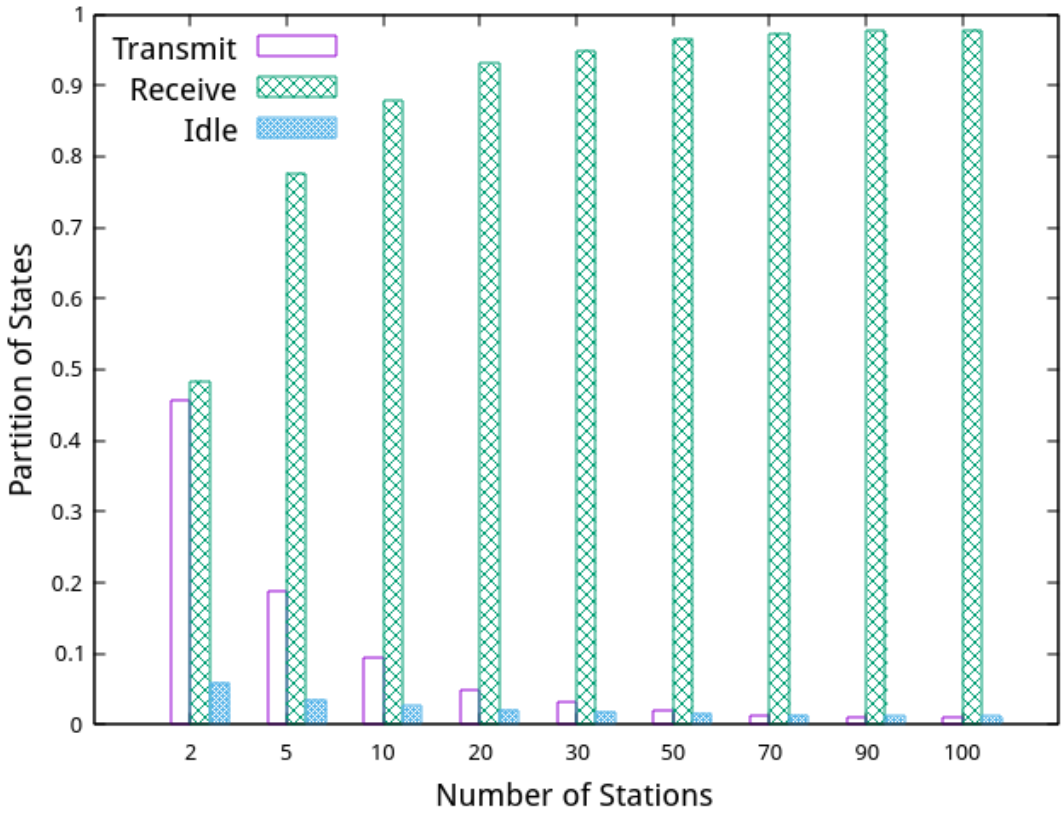

Figure 1.4: Partition of working states of a station under saturated condition

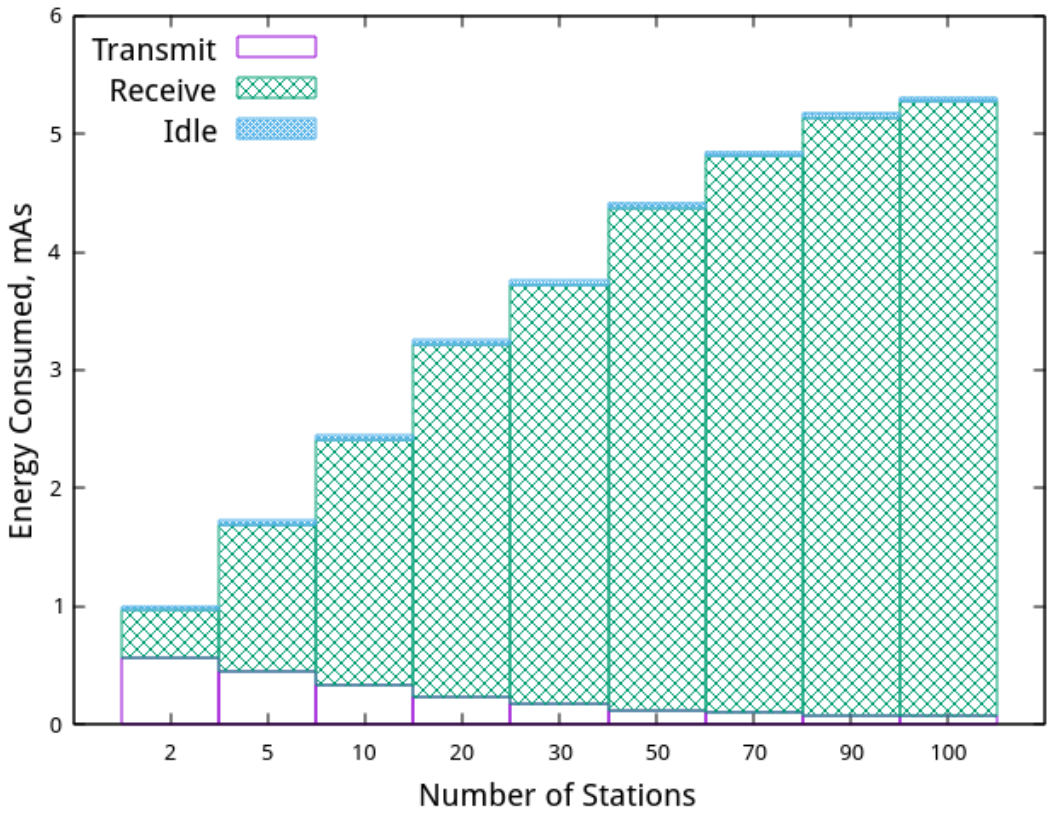

Figure 1.5: Energy consumption of a station under saturated condition

doi:10.6342/NTU201700509

the unfair queueing problem will worsen the effect of instability of DCF, leading to more waste of bandwidth and energy.

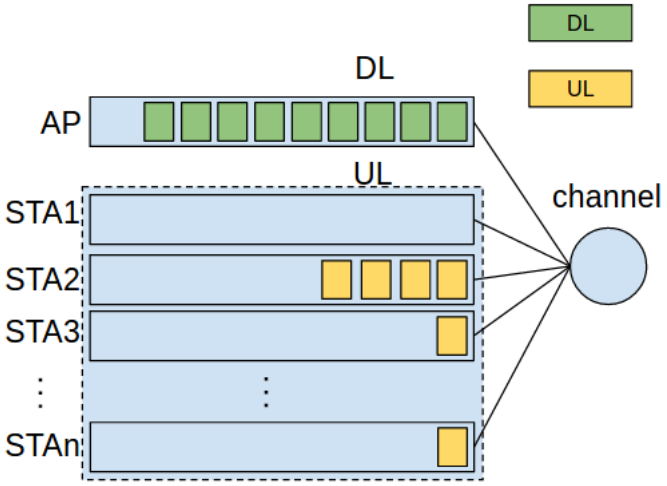

Figure 1.6: Unfair queueing problem of BSS

1.3 Solution: 802.11ax

The task group 802.11ax (TGax) aims at high efficient WLAN (HEW) especially for dense scenario. The TGax Project Authorization Request (PAR) [16] states that ”enable at least one mode of operation capable of supporting at least four times improvement in the average throughput per station in a dense scenario, while maintaining or improving the power efficiency per station.” To achieve the goal, the TGax makes revolutionary modifications on both PHY and MAC layers.

On the PHY layer, OFDMA [17] is firstly adopted by 802.11 to implement multi-user (MU) PHY for both DL and UL transmissions, namely AP could communicate with multiple stations simultaneously. The MU-OFDMA enables both MU DL and MU UL, and MU UL is more complicated for the stringent time synchronization. Thus, correspondingly see Fig. **??**, a new control frame is created called trigger frame (TF) to initiate a MU UL transmission[1]. This TF-based MU UL mechanism permits AP as central controller to schedule both DL and UL transmission, which transfers the distributed access protocol to a centralized access protocol. In this way, 802.11ax’s MAC will not be a distributed random access mechanism and unfair queueing problem could be resolved inherently.

doi:10.6342/NTU201700509

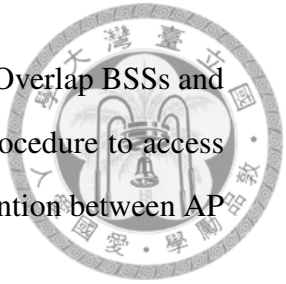

Actually, the new MAC is based on DCF since it helps co-exist among Overlap BSSs and other systems. The difference is that only AP needs to follow DCF procedure to access channel, while HE-STA (802.11ax STA) is scheduled by AP. The contention between AP and stations doesn't exist any more.

Though AP does not need to contend with stations, random access for non-AP stations are still necessary for its high efficiency on transmitting short packets. Thus, with the MU-OFDMA PHY, a multi-channel random access, OFDMA-based random access (OBRA), is proposed in the 802.11ax standard draft [1]. It could be exploited as an efficient way for stations to initiate a traffic stream by sending bandwidth request. Detailed illustration of 802.11ax features is in chapter 2.

1.4 Related Works

Random access in radio network starts from single channel Aloha [18], and [19] enhance the Aloha by slotting the time duration. Carrier sense multiple access (CSMA), also reducing collisions, is later analyzed by [20]. Random access mechanism is important for transmitting short packets [13], it thus exists in current radio networks.

Since 802.11 WLAN is widely accepted in recent decades, the evaluation of the 802.11 MAC efficiency is a fertile field along with the evolution of 802.11 MAC. The fundamental of 802.11 MAC DCF, which does not change during the last decades for its robustness and simplicity, bases on a random access mechanism CSMA/CA. Also centralized control scheme like point coordination function (PCF) is issued in 802.11 but is not widely accepted by industry. [21] has discussed the MAC alternatives for WLAN before the release of 802.11 specification. Various methods were proposed to analyze the MAC efficiency during the last decades. In [22][23] and [24], assuming backoff time follows a geometric distribution, an analytical formula for the protocol capacity namely throughput of DCF is derived and [24] proposed a distributed algorithm to tune its backoff algorithm at run-time. In [14], Bianchi proposed a simple and accurate model, which is a discrete-time bi-dimention Markov chain model, to compute the throughput of DCF under saturated condition and ideal channel assumptions. Afterward, this model is extended

doi:10.6342/NTU201700509

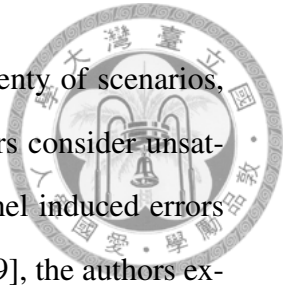

to evaluate throughput and delay performance of DCF or EDCA in plenty of scenarios, which validate the accuracy of the model. In [25] and [26], the authors consider unsaturated condition by introducing a new idle state. The impact of channel induced errors and capture effects is also evaluated in [26][27][28][29]. In [30] and [19], the authors extend Bianchi's model accounting most features of EDCA in 802.11e under ideal channel condition.

Standardization of next generation WLAN 802.11ax [1] is almost complete, exploiting therein MU-OFDMA PHY and a centralized MAC scheme. However, the new random access, OBRA is proposed in [1] as a multi-channel slotted Aloha with exponential backoff algorithm, transforming SU to MU channel. The multi-channel random access was studied by [31][32][33][34][35] at first, [32] calculating the stability region, [35] using Markov model to analyze throughput and delay of multi-channel slotted Aloha with or without reservation. In [36], a dynamic reservation technique, also called split channel, is introduced and analyzed. [37][38] evaluate the maximum achievable throughput of split-channel MAC schemes that are based on the RTS/CTS dialogue and that rely on pure Aloha or on CSMA. However, the split-channel MAC scheme is different from multi-channel slotted Aloha.

Multi-channel slotted Aloha is implemented by 802.11 WLAN for the first time, while it has been adopted by cellular networks for a while to perform initial association and to request transmission resource. For 802.11 WLAN, one of few works [39] generalizes CSMA/CA to MU-OFDMA, which is very different from the OBRA defined in 802.11ax [1]. Most focus on cellular networks, like 3GPP LTE-A and IEEE 802.16. In the literature, works follow the research of single channel slotted Aloha [19], working on stability [40], closed-form expression of throughput [41][40][42], collision probability [43][44], and access delay [41][43][44] of multi-channel slotted Aloha. [40] stabilizes multi-channel slotted Aloha by pseudo-Bayesian algorithm. Collision resolution including uniform backoff and exponential backoff is investigated, [41][44] comparing the impact of both two backoff algorithms, while [43] considering only exponential backoff. And [42] designs a 1-persistent type retransmission that avoids backoff to achieve a fast access. Different from

doi:10.6342/NTU201700509

above works on steady-state performance, Wei [45][46] conducts a transient-performance analysis of OFDMA system with busty traffic.

As far as we know, no closed-form of performance analysis of the OBRA has been derived, and the Markov chain model has never been used to model the multi-channel slotted Aloha.

1.5 Motivation

Though 802.11 MAC efficiency has been investigated deeply, the new OBRA is absolutely different from legacy 802.11 DCF-like MAC scheme. And no closed-form expression of the throughput or delay performance of the OBRA has been derived. In the literature of multi-channel slotted Aloha, the methods used are not as accurate as the [14] for DCF. And differences still exist between the applied multi-channel Aloha and the OBRA of 802.11ax. Since [14] proposes an accurate and simple bi-dimensional Markov chain model depicting every details of CSMA/CA, we are extending the model from SU channel to multi-channel slotted Aloha. According to [14], the saturated analysis, which predicts the steady-state behavior, helps obtain some insight of the mechanism, including the impact of the system parameters.

1.6 Organization

The thesis is organized as follows. More explanations of 802.11ax features are given in Section 2.1. In Section 2.2, a detailed illustration of OFDMA-based random access procedure is presented. Chapter 3 contains the system model and derivation of two metrics, including system efficiency and access delay. Simulation which helps validate the system model is presented in this chapter. Then Chapter 4 is the performance evaluation of optimal performance and checks the impact of system parameters on performance. Chapter 5 remains the conclusion remark and future work.

doi:10.6342/NTU201700509

Chapter 2

802.11ax Features

Some necessary features of 802.11ax to better understand the OBRA mechanism are illustrated in this section. First, MU-OFDMA is firstly adopted by 802.11 to implement MU DL and MU UL. To support MU UL, study group 802.11ax proposes trigger-based MU UL procedure, which means UL transmission could be scheduled by AP, shifting distributed coordination to centralized control. Then OFDMA-based random access (OBRA) is illustrated in the following subsection. For more features of 802.11ax, refer to [1][47].

2.1 MU-OFDMA

OFDM has been proposed as one of the prime schemes for MU communications. In such OFDM-based systems, the total bandwidth is divided into multiple sub-channels so that multiple access can be accommodated in an OFDMA. Though MU PHY has been implemented in 802.11n and 802.11ac with MU-MIMO, only MU DL transmission is realized. MU-OFDMA implements both MU DL and MU UL. Especially for MU UL transmission, which is more difficult to implement, trigger-based MU UL is thus proposed.

With MU PHY, the original SU 20 MHz channel could be specified more fine-grained and be also aggregated to a wider channel to meet various bandwidth demands. The resource unit (RU), which can be accessed by one STA, is specified as Table 2.1. For example, the smallest RU is 26-tone, with which a 20 MHz could be separated into 9 subchannels. Also multiple 20 MHz channels can be aggregated to improve system throughput,

doi:10.6342/NTU201700509

which is referred to as *Channel Bonding*. It is worth mentioning that every transmission of MU should end at the same time. That means padding is required for shorter packets.

Table 2.1: Maximum number of RUs for each channel width

RU type	CBW20	CBW40	CBW80	CBW80+80 and CBW160
26-tone RU	9	18	37	74
52-tone RU	4	8	16	32
106-tone RU	2	4	8	16
242-tone RU	1	2	4	8
484-tone RU	N/A	1	2	4
996-tone RU	N/A	N/A	1	2
2×996 tone RU	N/A	N/A	N/A	1

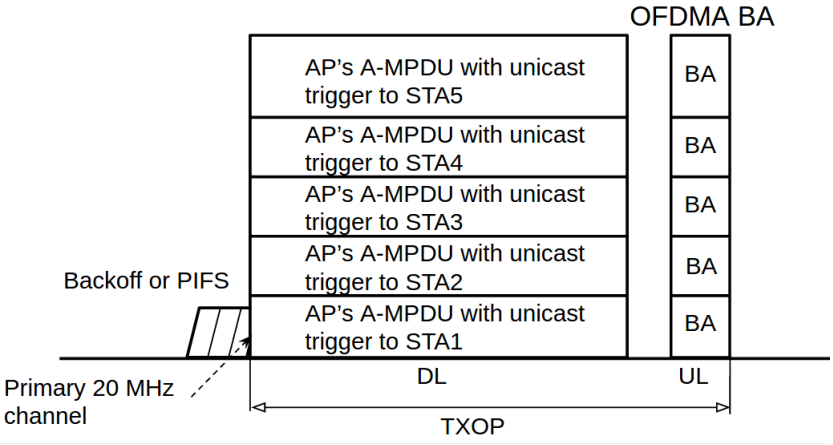

Figure 2.1: MU DL of 802.11ax

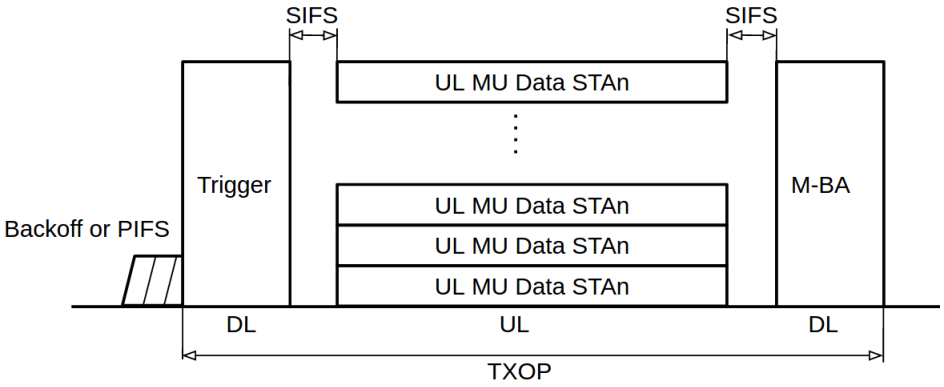

Figure 2.2: Trigger-based MU UL of 802.11ax

In respect of MAC layer, first, for MU DL transmission, AP transmits DL packets to multiple stations simultaneously as in Fig. 2.1. Secondly, MU UL transmission is more complicated because WiFi network is not a well-synchronized system. A trigger-based

doi:10.6342/NTU201700509

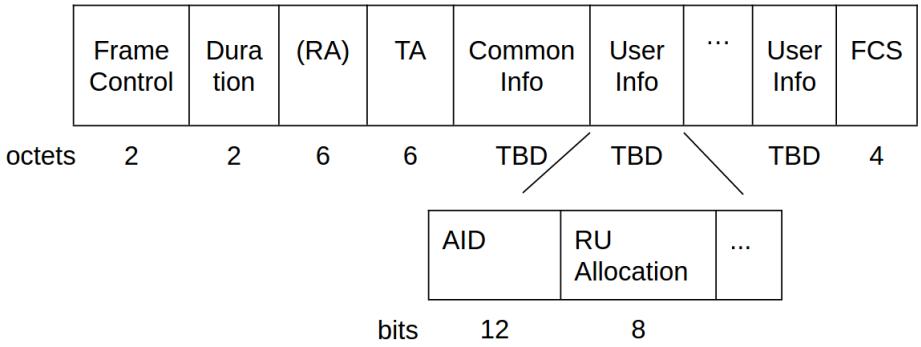

Figure 2.3: Trigger Frame format

MU UL transmission is thus issued in Fig. 2.2. A brand new control frame, trigger frame (TF), is created to be transmitted by AP to initiate the UL transmission. STAs could not transmit UL packets until they receive a TF which allocates RU for the STA or specifies RUs for random access. Afterwards, AP responds with ACK frame. All the procedure form a three-way handshake UL transmission. The trigger frame format is in Fig. 2.3. Since the standard is in progress, some fields remain to be determined (TBD). In the field *User Info*, subfield *AID* represents the identification of STA and subfield *RU Allocation* represents the RU allocated to the STA. Especially, *AID* with value 0 means the RU is for random access.

2.2 802.11ax Random Access Illustration

An example of TF-based MU UL transmission with OBRA, illustrated in Fig. 2.4, is divided into two steps, one as random access procedure and the other UL data transmission. The random access procedure, namely the OBRA, is initiated by AP to collect traffic information named buffer state report (BSR) from stations. Thereby in the next step, the AP could allocate RUs to STAs by transmitting a TF containing RU allocation. Then the STAs, receiving the TF with resource allocation information, transmit UL data packets. And AP at last responds ACK. Therefore, TFs in the example have two variants, one for random access and the other for resource allocation. When traffic information is collected, the allocation is beyond the scope of this paper. Only step one is our interest.

Details of OBRA mechanism is as Fig. 2.5. To initialize a random access procedure,

doi:10.6342/NTU201700509

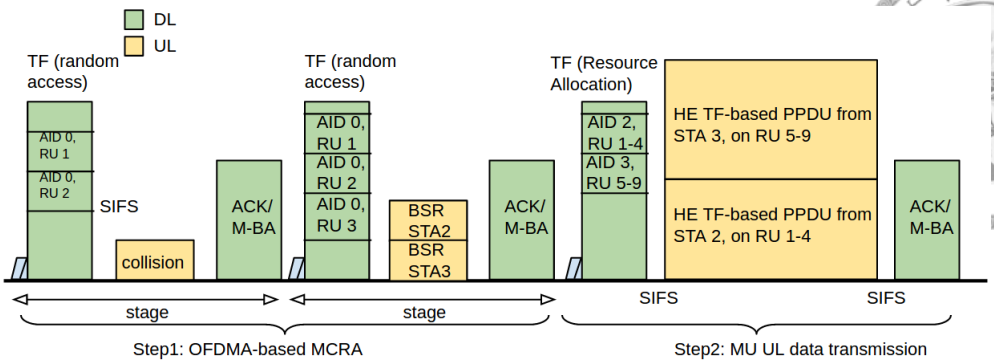

Figure 2.4: An example of Trigger-based MU UL transmission with OBRA

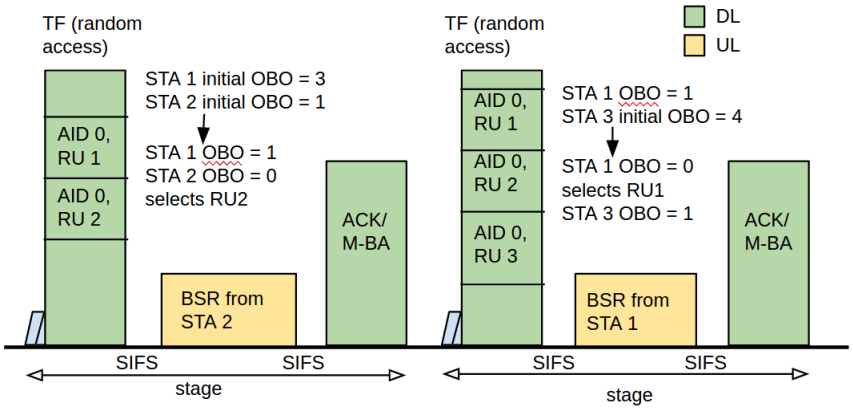

Figure 2.5: Illustration of OBRA

AP first transmits a TF announcing RUs for random access by setting the AID of the RUs to 0. Attempting STAs, whose buffers are not empty, maintain a backoff counter named OFDMA Backoff (OBO), which are randomly generated among range $[0, OCW]$. Then the OBO subtracts the value of M once receiving the TF, otherwise freezes, where M is calculated by sum the number of RUs whose AID equals 0. When the OBO reaches 0, the STA will randomly select a RU from those whose AIDs equal 0 to transmit a request after short inter-frame spacing (SIFS). After that, AP responds with a block-ACK indicating which STAs contend successfully. The period of the whole three-way handshaking is named a *stage*. A successful stage means at least one STA contend successfully to transmit a request in a stage. It is worth noting that the stage in this paper, which is specified from standard [1], is a concept of the time interval, not the backoff stage in other papers. To avoid confusion of the two meanings, backoff stage is replaced with *backoff level* in this paper. When STAs fail to contend, the OCW will be doubled until OCW reaches OCW_{max}, which means the backoff level increases one step once a failure until

doi:10.6342/NTU201700509

the highest level.

In terms of implementation, system parameters of the OBRA are configured dynamically by AP, including OCW_{min}, OCW_{max}, M, where OCW_{min}, OCW_{max} represent the minimum and the maximum contention window, and M as the number of RUs for random access. Two of critical parameters OCW_{min}, OCW_{max} are configured in Random Access Parameter Set (RAPS) element contained in beacon frame sent by AP. Check field *OCW Range* in RAPS element as in Fig. 2.6, $OCW_{min} = 2^{EOCW_{min}} - 1$, $OCW_{max} = 2^{EOCW_{max}} - 1$. M is obtained from TF by sum the number of RUs whose *AID* equal 0. To simplify following analysis, we issue another parameter m, *maximum backoff level*, so that $OCW_{max} = (OCW_{min} + 1) * 2^m - 1$. The configuration of system parameter is absolutely different from that of legacy 802.11, where all the parameters are predefined in each STA's hardware. OBRA is thus more flexible compared with DCF.

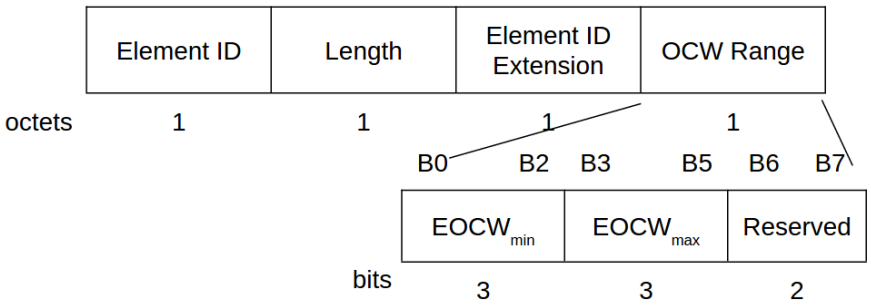

Figure 2.6: Random Access Parameter Set (RAPS) Element

doi:10.6342/NTU201700509

Chapter 3

System Model

The bi-dimensional Markov chain model of DCF, first proposed by Bianchi [14], depicts every details of the CSMA/CA, including binary exponential backoff. One of main contribution of this thesis is extending the bi-dimensional Markov chain model to conduct the saturation analysis of 802.11ax OFDMA-based random access, under assumptions of ideal channel conditions, no hidden terminals, and a constant and independent collision probability regardless of the number of retransmissions. We assume a single-BSS scenario where there are n stations and one AP. Each stations are saturated, namely always non-empty queue. Since the OBRA is a random access for stations except AP, thus traffic from AP i.e. DL is not considered. What's more, see Fig. 2.4 and Fig. 2.5, the UL data packets transmissions are ignored, only OBRA for bandwidth request considered.

The analysis is divided into three parts. First is the bi-dimensional Markov chain model to estimate the packet transmission probability τ and conditional collision probability p. Secondly, we evaluate some metrics as function of τ, including the number of successful contending stations in a stage n_s, self-defined system efficiency *eff*, and access delay of a STA D. Thirdly, results of simulations are displayed to verify the accuracy of the new bi-dimensional Markov chain model. Table 3.1 is a list of all parameters and notations.

To better understand the validation of the bi-dimensional Markov Chain model for the OBRA, we need to clarify concept of time of OBRA. The whole procedure of OBRA,a three-way handshake, is so-called *stage*. In legacy 802.11 DCF, time is measured in *slot*.

doi:10.6342/NTU201700509

Table 3.1: Parameters and Notations Interpretation

Notations	Meaning
n	Number of stations
OCW_{min} (W_0)	Minimum OFDMA contention window
OCW_{max} (W_m)	Maximum OFDMA contention window
M	Number of RUs for random access
m	Maximum backoff level
p	Packet collision probability
τ	Station's transmission probability
n_s	Number of successful stations in a stage
D	Access delay, number of stages for a station to contend successfully
D_s	Number of stages until a successful stage

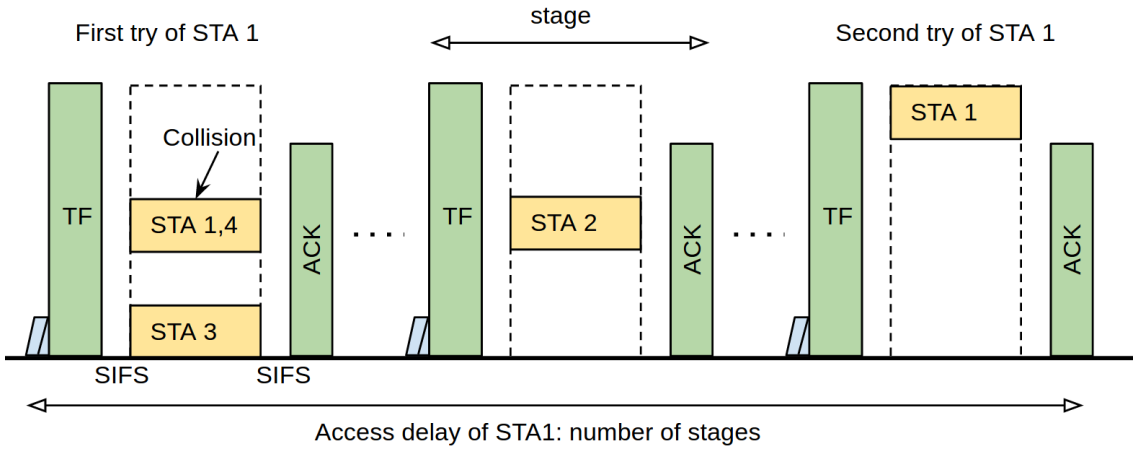

Figure 3.1: Concept of time in OFDMA-based random access

Here, time is measured in stage, which is also a discrete time and is not synchronized with physical time. Stages could thus be mapped with slots in legacy random access mechanism, see 3.1. Then, access delay is calculated in number of stages for station to access channel.

3.1 Packet Transmission Probability

Consider a single BSS with an AP and n of STAs under saturation condition, i.e. every STA with always non-empty queue. Also, the ideal channel is assumed so that collision happens only if more than one station transmits at the same RU. Only UL BSR transmission (bandwidth request) is concerned, while DL transmission and UL data transmission are ignored here.

doi:10.6342/NTU201700509

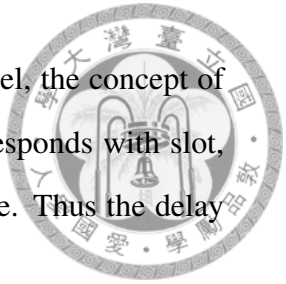

At first, to model OBRA with the discrete-time Markov chain model, the concept of time is supposed to be changed. In DCF, time unit of the model corresponds with slot, while in OBRA time unit of the model is stage, a three-way handshake. Thus the delay will be measured in the number of stages.

Similar to Bianchi's work, let $\{s(t), b(t)\}$ be the bi-dimension process, where $s(t)$ denotes the backoff level $(0, \cdots, m)$, and $b(t)$ denotes backoff counter $(0, \cdots, W_i)$. With the discrete and integer time scale, t and $t+1$ corresponds to beginnings of two consecutive stages. $\{b(t)\}$ is not a Markov process because the state of the current stage depends on the history of transmission instead of only the previous stage. The bi-dimensional process $\{s(t), b(t)\}$ is a Markov chain. The key assumption is still necessary that at each request transmission, and regardless of the number of retransmission suffered, each request frame collides with constant and independent probability p. With the independence assumption, p will be a constant. Then the Markov chain is able to be conducted as in Fig. 3.2.

Another important difference between the two Markov chain models of OBRA and DCF, is clarified here. Since the station of DCF senses the carrier before transmitting, it will freeze its backoff counter and stay at the state if channel is sensed busy. However in the OBRA, because the time unit, a stage, contains a period for exactly a packet transmission, backoff of stations i.e. OBO certainly subtract M only if a TF for random access is received. Stations of the OBRA thus stay in one state for a period of exactly single stage and transform to another state in next stage.

Some modifications are mentioned here to adapt to differences between OBRA and DCF. First, in a row of states, as OBO subtracts the value of M rather than 1, stations transfer to states M-step ahead. Second, since states with $b(t) \leq M$ will decrease to 0 at the current state, which means stations could access RUs, we could merge these states into one state, denoted by $\{i, T\}$. T is an integer set of $[0, M]$.

Let's assume $P\{i_1, k_1 | i_0, k_0\} = P\{s(t+1) = i_1, b(t+1) = k_1 | s(t) = i_0, b(t) = k_0\}$.

doi:10.6342/NTU201700509

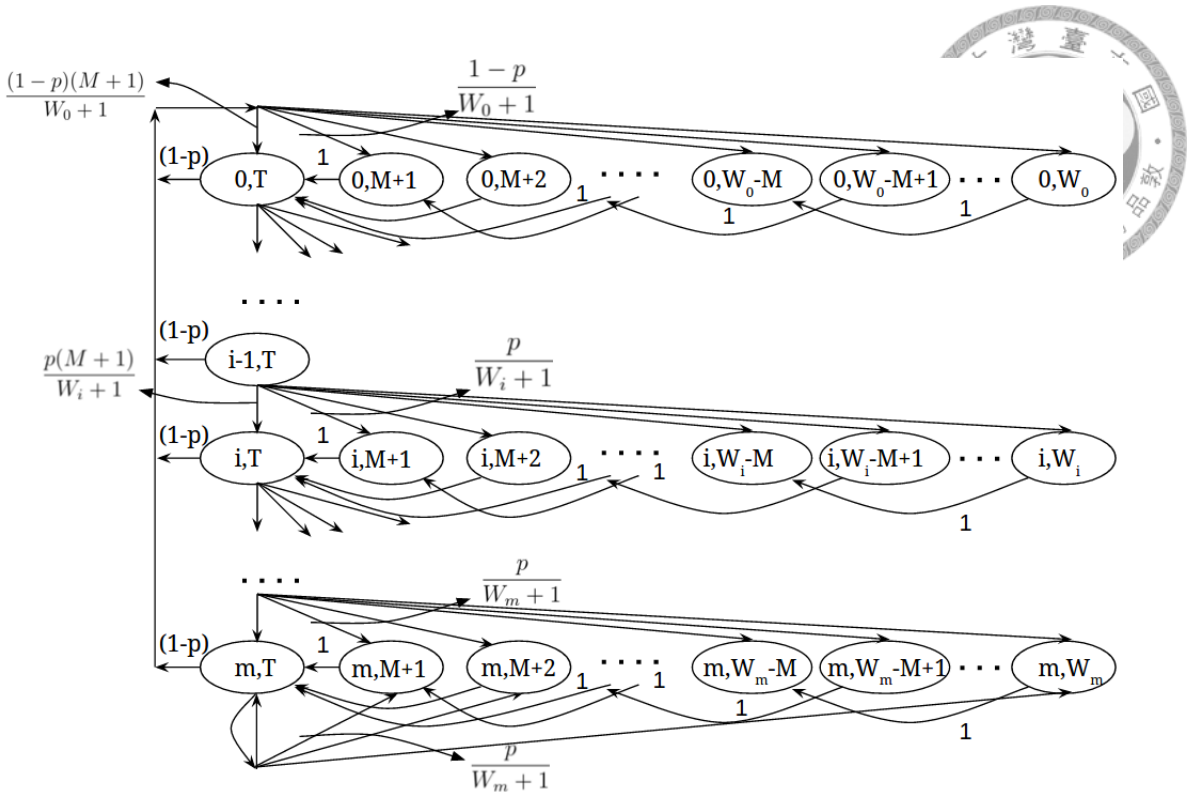

Figure 3.2: Markov Chain model for the backoff window size

In this Markov Chain, the only non null one-step transition probabilities are

$$\begin{cases} P\{i,T|i,k\}=1 & k\in[M+1,2M] \quad i\in[0,m] \\ P\{i,k-M|i,k\}=1 & k\in[2M+1,W_i] \quad i\in[0,m] \\ P\{0,k|i,T\}=\frac{1-p}{W_0+1} & k\in[M+1,W_0] \quad i\in[0,m] \\ P\{0,T|i,T\}=\frac{(1-p)(M+1)}{W_0+1} & \quad i\in[0,m] \\ P\{i,k|i-1,T\}=\frac{p}{W_i+1} & k\in[M+1,W_i] \quad i\in[1,m] \\ P\{i,T|i-1,T\}=\frac{p(M+1)}{W_i+1} & \quad i\in[1,m] \\ P\{m,k|m,T\}=\frac{p}{W_m+1} & k\in[M+1,W_m] \\ P\{m,k|m,T\}=\frac{p(M+1)}{W_m+1} & \end{cases} \tag{3.1}$$

The first and second equations in (3.1) accounts for the fact that the backoff counter maintained by stations will subtract M, the number of RUs for random access. The third and fourth equations represent that after a successful contention, stations will reset the contention window size to initial window size and uniformly generate a backoff value among $[0, W_0]$, since T is an integer set $[0, M]$, the transition probability to states $\{i, T\}$

doi:10.6342/NTU201700509

is $M+1$ times of that to states $\{i,k\}$. For the fifth and sixth equations, they represent when a failure contention occurs, the contention window size will be doubled, $W_i = 2W_{i-1}+1$. The last two equations are the case of failure at the maximum backoff level. We assume no packets are discarded, repeating retransmitting until success.

Let $b_{i,k} = \lim_{t\to\infty} P\{s(t)=i, b(t)=k\},\ i \in [0,m],\ k \in [0,W_i]$, be the stationary distribution of the Markov chain. Then we show how to obtain transmission probability τ and conditional collision probability p. First, for states with $b(t)=T$, in which stations will transmit requests or BSRs in current stage,

$$b_{i-1,T}\cdot p = b_{i,T} \to b_{i,T} = p^i b_{0,T}, \quad 0 \le i < m \tag{3.2}$$

$$b_{m-1,T}\cdot p = (1-p) b_{m,T} \to b_{m,T} = \frac{p^m}{1-p} b_{0,T}. \tag{3.3}$$

Then, the other states could be expressed by states with $b(t)=T$:

$$b_{i,k} = \begin{cases} (\lfloor \frac{W_0-k}{M} \rfloor + 1)\frac{(1-p)}{W_0+1}\sum_{i=0}^{m} b_{i,T}, & M+1 \le k \le W_0,\ i=0 \\ (\lfloor \frac{W_i-k}{M} \rfloor + 1)\frac{p}{W_i+1} b_{i-1,T}, & M+1 \le k \le W_i,\ 0<i<m \\ (\lfloor \frac{W_m-k}{M} \rfloor + 1)\frac{p}{W_m+1}(b_{m-1,T}+b_{m,T}), & M+1 \le k \le W_m,\ i=m \end{cases} \tag{3.4}$$

The first and third subequation in (3.4) are first and last row of states in Fig. 3.2 except the first column state with $b(t)=T$. The second subquation is the states in the middle rows without the states in the first column. From (3.3), $\sum_{i=0}^{m} b_{i,T} = \frac{b_{0,T}}{1-p}$ is obtained; whereby each row of states in Fig. 3.2 could be obtained by summing the subequations of (3.4) respectively to get (3.5).

$$\begin{cases} \sum_{k=M+1}^{W_0} b_{0,k} = \frac{b_{0,T}}{W_0+1}\left(-\frac{M}{2}\left\lfloor\frac{W_0}{M}\right\rfloor^2 + \left(W_0-\frac{M}{2}\right)\left\lfloor\frac{W_0}{M}\right\rfloor\right) \\ \sum_{i=1}^{m-1}\sum_{k=M+1}^{W_i} b_{i,k} = \frac{b_{0,T}}{W_0+1}\left(\frac{p}{2}\right)^i\left(-\frac{M}{2}\left\lfloor\frac{W_i}{M}\right\rfloor^2 + \left(W_i-\frac{M}{2}\right)\left\lfloor\frac{W_i}{M}\right\rfloor\right) \\ \sum_{k=M+1}^{W_m} b_{m,k} = \frac{b_{0,T}}{W_0+1}\frac{(\frac{p}{2})^m}{1-p}\left(-\frac{M}{2}\left\lfloor\frac{W_m}{M}\right\rfloor^2 + \left(W_m-\frac{M}{2}\right)\left\lfloor\frac{W_m}{M}\right\rfloor\right) \end{cases} \tag{3.5}$$

doi:10.6342/NTU201700509

Each subequation in (3.5) has the same term: $-\frac{M}{2}\left\lfloor\frac{W_i}{M}\right\rfloor^2+\left(W_i-\frac{M}{2}\right)\left\lfloor\frac{W_i}{M}\right\rfloor$. To simplify the expression, let $X_i=-\frac{M}{2}\left\lfloor\frac{W_i}{M}\right\rfloor^2+\left(W_i-\frac{M}{2}\right)\left\lfloor\frac{W_i}{M}\right\rfloor$. Then, sum the steady state probability of all states to get (3.7).

$$1=\sum_{i=0}^{m}\sum_{k=0}^{W_i}b_{i,k}=\frac{b_{0,T}}{W_0+1}\left(X_0+\sum_{i=1}^{m-1}X_i\left(\frac{p}{2}\right)^i+X_m\frac{\left(\frac{p}{2}\right)^m}{1-p}\right)+\frac{b_{0,T}}{1-p} \tag{3.6}$$

$$=b_{0,T}\left(\frac{(1-p)X_0+(1-p)\sum_{i=1}^{m-1}X_i\left(\frac{p}{2}\right)^i+X_m\left(\frac{p}{2}\right)^m+W_0+1}{(W_0+1)(1-p)}\right) \tag{3.7}$$

Therefore, τ, the probability of a station transmitting a request at a stage, could be expressed by

$$\begin{aligned}\tau&=\sum_{i=0}^{m}b_{i,T}=\frac{b_{0,T}}{1-p}\\&=\frac{W_0+1}{W_0+1+(1-p)X_0+(1-p)\sum_{i=1}^{m-1}X_i\left(\frac{p}{2}\right)^i+X_m\left(\frac{p}{2}\right)^m}\end{aligned} \tag{3.8}$$

As a side note, it is interesting to highlight that, when $m=0$ (i.e., no exponential backoff is considered), check equation 3.6, the terms containing $X_i, i>0$ will disappear, and $b_{0,T}/(1-p)$ will just be $b_{0,T}$. Thus, equation 3.7 will be degraded to

$$1=b_{0,T}\left(\frac{W_0+1+X_0}{W_0+1}\right), \tag{3.9}$$

further simplified that $M=1$ and $X_0=\frac{W_0^2-W_0}{2}$, then

$$\begin{aligned}\tau=b_{0,T}&=\frac{W_0+1}{W_0+1+X_0}\\&=\frac{2(W_0+1)}{W_0^2+W_0+2},\end{aligned} \tag{3.10}$$

which is different from that of CSMA/CA with constant window size [22], where $\tau=\frac{2}{W_0+1}$. That is because stations of CSMA/CA freezes backoff counter when sensing busy channel while no such freeze mechanism of backoff counter exists in OBRA.

On the other hand, in general, τ depends on the conditional collision probability p, which is still unknown. To find the value of p it is sufficient to note that the probability

doi:10.6342/NTU201700509

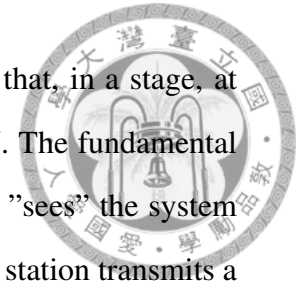

p that a transmitted packet encounters a collisions, is the probability that, in a stage, at least one of the $n-1$ remaining stations transmit on the selected RU. The fundamental independence assumption given above implies that each transmission "sees" the system in the same state, i.e., the steady state. At steady state, each remaining station transmits a packet with probability τ. This yields

$$p = 1 - \left(1 - \frac{\tau}{M}\right)^{n-1}. \tag{3.11}$$

Rewrite the (3.11), $\tau^{\star} = \left(1 - (1-p)^{\frac{1}{n-1}}\right) M$. To obtain transmission probability τ and conditional probability p, we need to find solutions to group of equations 3.8 and 3.11. $\tau^{\star}(p)$ is a monotonically increasing function. Though $\tau(p)$ is hard to determine the monotonicity from the expression of equation 3.8 with respect to p. We justify the monotonic decrease of function 3.8 with numerical method. Also, $\tau(0) = \frac{W_0+1}{W_0+1+X_0} > \tau^{\star}(0) = 0$. And $\tau(1) < \tau^{\star}(1) = M$. We find the only solution with numerical method.

3.2 Random Access Efficiency

With the transmit probability, we could easily estimate efficiency of random access mechanism. Firstly, find expected number of stations who succeed in contending to transmit request at a stage, which is denoted with $E[n_s]$. Extending n_s, we define a system efficiency as an important metric. Secondly, we are interested in the access delay of request frame. In another word, say how many stages needed for a station to succeed in contending, denoted by D. What's more, another interesting metric is how many stages are elapsed until a successful stage, which means at least one station succeed in contending in the stage. This metric is a concept similar to "delay" in the second use case of OFDMA-based random access. We represent it with D_s. It helps design whole MU UL transmission procedure. Here, our concern is mainly on n_s, system efficiency and access delay all of which are purely related to random access procedure. The other metric D_s is only expressed in the subsection of access delay, not being discussed later.

doi:10.6342/NTU201700509

3.2.1 n_s and System Efficiency

What we care in the random access is that how many stations contend successfully in a single stage, denoted by n_s. Given transmission probability τ and conditional collision probability p, we could obtain probability that a station succeeds in contending in a stage, $P_{s\_station} = \tau(1-p)$. Then, with equation 3.11, $E[n_s]$ is easily computed as follows.

$$\begin{aligned} E[n_s] &= nP_{s\_station} \\ &= n\tau(1-p) \\ &= n\tau(1-\frac{\tau}{M})^{n-1} \end{aligned} \tag{3.12}$$

Furthermore, normalizing n_s so that we could compare among different M, thus system efficiency is defined as the ratio between the number of successful stations in a given stage and the M.

$$\begin{aligned} \textit{eff}\,(\tau) &= \frac{E[n_s]}{M} \\ &= \frac{n\tau(1-\frac{\tau}{M})^{n-1}}{M}. \end{aligned} \tag{3.13}$$

Both two metrics are our concerns. Another metric, access delay, is derived in next subsection. With all these metrics, we could evaluate the performance later.

3.2.2 Access Delay

Access delay D is defined as number of stages needed for a station to succeed in contending. This access delay is different from legacy access delay since the concept of time here is not corresponding with physical time. We measure the time as number of stages. Access delay D follows geometric distribution with parameter $P_{s\_station}$, which is obtained just now. Thus the expected value of access delay of request frame, $E[D]$, is

$$E[D] = \frac{1}{P_{s\_station}} = \frac{1}{\tau(1-\frac{\tau}{M})^{n-1}}. \tag{3.14}$$

doi:10.6342/NTU201700509

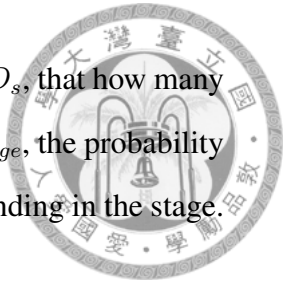

Then another interesting metric which is not our focus, denoted by D_s, that how many stages are elapsed until a successful stage. We could firstly obtain P_{s_stage}, the probability of a successful stage, which means at least one station succeed in contending in the stage.

$$\begin{aligned} P_{s\_stage} &= 1 - P\{n_s = 0\} \\ &= 1 - (1 - P_{s\_station})^n \\ &= 1 - (1 - \tau(1-p))^n \end{aligned} \tag{3.15}$$

Since D_s follows geometric distribution with parameter P_{s_stage},

$$\begin{aligned} E[D_s] &= \frac{1}{P_{s\_stage}} \\ &= \frac{1}{1 - (1 - \tau(1-p))^n} \end{aligned} \tag{3.16}$$

In a word, we focus on three metrics: number of successful stations in a stage by n_s, system efficiency by $E[n_s]/M$ and access delay given by D. Actually, only two variables are concerned, n_s and D. However, n_s and its normalized value are both meaningful, which we will explain in following sections.

3.3 Model Validation

As Fig. 2.5, only OBRA mechanism is considered. We carry out comprehensive simulations implemented by an event-driven customized simulation program, written in C language. The important parameters are set as in table 3.1. Simulation runs with three-way handshake stage by stage for 1,000,000 stages with a variety of parameter sets $\{M, OCW_{min}, OCW_{max}\}$. We collect the information of the two variables, the number of successful attempt STAs n_s and expected access delay D. The values of results from both analysis and simulation are given in Fig. 3.3 and Table 3.2, showing that the Markov model precisely predicts the steady state behavior of the OBRA mechanism.

doi:10.6342/NTU201700509

Table 3.2: Analysis versus simulation: n_s and access delay with $m = 3, M = 9, OCW_{min} = 15$

n_s	analysis	simulation
$n = 1$	0.72727	0.72741± 0.01
$n = 5$	2.23001	2.23051± 0.01
$n = 10$	2.88954	2.88421± 0.01
$n = 20$	3.29798	3.29903± 0.01
delay	analysis	simulation
$n = 1$	1.37500	1.37473± 0.01
$n = 5$	2.24214	2.24939± 0.01
$n = 10$	3.46075	3.46715± 0.01
$n = 20$	6.06432	6.06238± 0.01

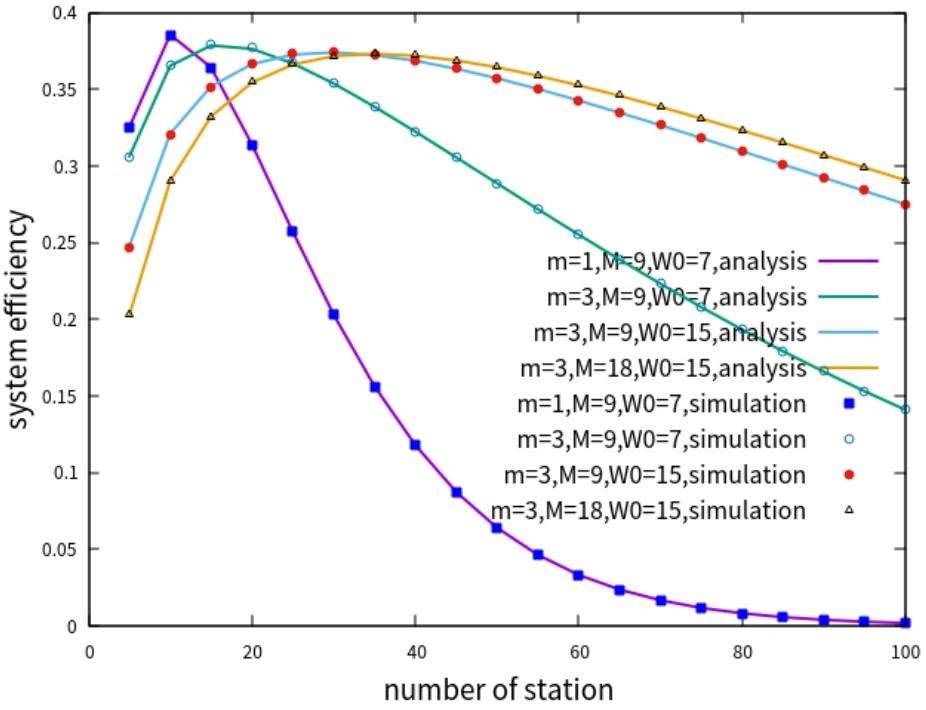

Figure 3.3: System efficiency: Analysis versus Simulation

doi:10.6342/NTU201700509

Chapter 4

Performance Evaluation

4.1 Maximum System Efficiency and Minimum Access Delay

With the system efficiency given in (3.13), we take the derivative with respect to τ, and find the extreme point, $\tau^\star = M/n$. Since $\tau \in [0, 1]$, $\tau^\star = min\{1, M/n\}$. What we care is when n, the number of contending stations, is large, i.e., $\tau^\star = M/n$. Then the system efficiency is

$$\textit{eff}\,(\tau^\star) = (1 - \frac{1}{n})^{n-1} \tag{4.1}$$

Then the maximum n_s is easy to generate.

$$E[n_s]^\star = M \cdot \textit{eff}\,(\tau^\star) = M(1 - \frac{1}{n})^{n-1} \tag{4.2}$$

Thus the limit of system efficiency, based on infinite n, is

$$\lim_{n\to\infty} \textit{eff}\,(\tau^\star) = \lim_{n\to\infty} (1 - \frac{1}{n})^{n-1} = \frac{1}{e} \tag{4.3}$$

With the delay analysis given in 3.14, we also take the derivative with respect to τ, and find the extreme point, $\tau^\star = M/n$. Again, $\tau^\star = min\{1, M/n\}$. When $n \geq M$, the

doi:10.6342/NTU201700509

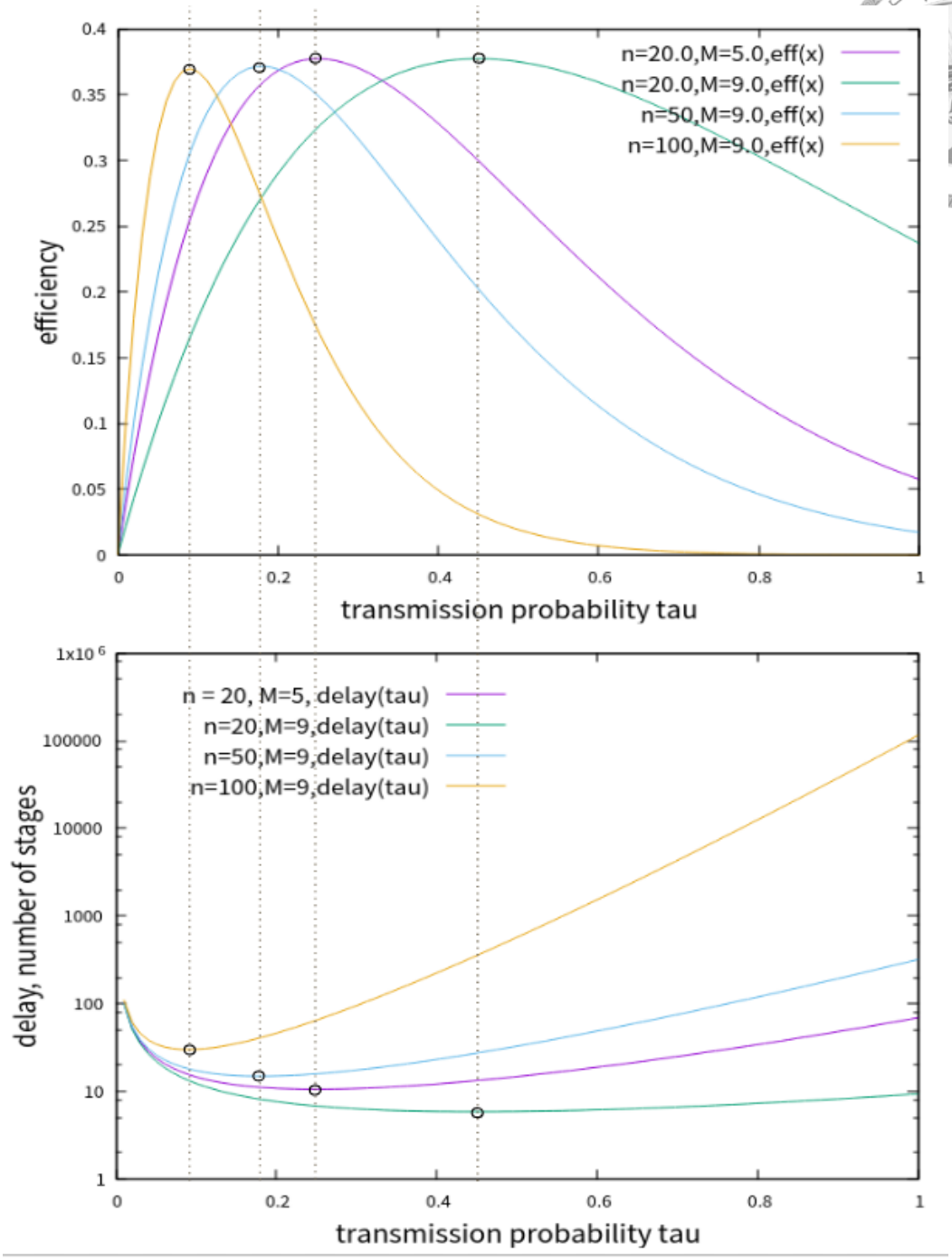

Figure 4.1: Efficiency and access delay versus transmission probability τ

minimum access delay is

$$D(\tau^{\star}) = \frac{n}{M(1-\frac{1}{n})^{n-1}}. \tag{4.4}$$

From above analysis, we find that the maximum system efficiency and minimum access delay are both obtained by the same transmission probability $\tau^{\star} = min\{1, M/n\}$.

doi:10.6342/NTU201700509

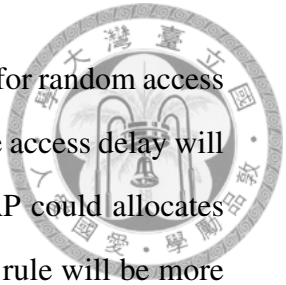

What's more, system efficiency is independent with M, number of RUs for random access in a stage, while M affects access delay. The larger M is, the shorter the access delay will be. It indicates that when AP allocates RUs for random access, the AP could allocates as many as possible, only if the channel of the RU is sensed idle. This rule will be more explained in next section.

Fig. 4.1 is plotted corresponding to (3.13) and (3.14). Consistent to the analysis above, the figure shows that the maximum system efficiency is independent of number of RUs for random access when $n \geq M$, and approaching to $1/e$ with n increasing. What's more, the optimal transmission probability τ of system efficiency and access delay is consistent with each other, which also validates the analysis.

According to (3.8) and (3.11), transmission probability τ depends on system parameters, M, W_0, m or W_m, and n. The only way to approach optimal performance is to employ adaptive techniques to tune the system parameter set $\{M, W_0, W_m\}$ on the basis of the estimated value of n. In the following section, we will evaluate the performance corresponding to different system parameters sets and propose the rules to tune the system parameter sets so that the transmission probability τ approach the optimal transmission probability, $\tau^\star$, which means both system efficiency and delay approach the optimal.

4.2 Effects of System Parameter

We have estimated the maximum system efficiency and minimum access delay in the previous section. Then we evaluate the metrics, n_s (number of stations who succeed in contending in a stage), system efficiency and D (access delay), under various parameter sets. With above analysis, we could evaluates transmission probability under various parameter sets, since the optimal transmission probability $\tau^\star$ means both maximum system efficiency and minimal access delay.

At last, we propose rules for configuring the parameter set $\{M, OCW_{min}, OCW_{max}\}$.

doi:10.6342/NTU201700509

4.2.1 RUs for Random Access M

(4.1) has indicated that M, has nothing to do with optimal system efficiency. However, n_s and D are proportional and inversely proportional to M respectively according to (4.2) and (4.4). Following analysis results validate the statement.

In Fig. 4.2a, the maximum system efficiency from various cases are almost the same, approaching $1/e$. The only difference is "where" the optimal point locates. Practically, the other two metrics, n_s and D, are closely related to M. Fig. 4.2b shows that larger M results in that more stations contend successfully in a stage. Moreover, Fig. 4.2c shows that larger M markedly reduce the access delay. Therefore, when AP allocates RUs for random access, AP should allocate as many RUs as possible.

4.2.2 Initial and max Contention Window (OCW_{min}, OCW_{max})

Fig. 4.3 shows case 1 ($M = 9$) and case 2 ($M = 18$), so that the rules we get are more convinced. In the figure, the purple line without point depicts the $\tau^\star$ that $\tau^\star = min\{1, M/n\}$. With above analysis and effects of M, we tune remaining parameters OCW_{min}, OCW_{max} so that τ approaches the optimal line. To see the trend of the line clearly, large and regular n are configured as in Fig. 4.3 and Fig. 4.4 so that rules are more evident.

First, the OCW_{min} or W_0, determines τ with small n. The larger W_0 is, the lower τ is at $n = 1$. That's why cases in Fig. 4.3 have two different start points, $W_0 < M$ share the same start point.

Secondly, $m = 0$ i.e., $W_0 = W_m$, results in constant τ, which is consistent with (3.10) that τ does not depend on n. Specially, $W_0 < M$ for scenario $n \leq M$, results in constant τ equals to 1, which perfectly matches $\tau^\star$ at $n \leq M$. Thus, if given $n \leq M$, the optimal configuration will be $OCW_{max} = OCW_{min} < M$.

Thirdly, performance of the dense scenario strongly depends on OCW_{max}. It determines the limit of the τ, i.e., where the line of τ will converge. And both the two figures in Fig. 4.3 correspond with the above statement. And larger W_m causes lower τ, which is closer to $\tau^\star$ when n is large.

doi:10.6342/NTU201700509

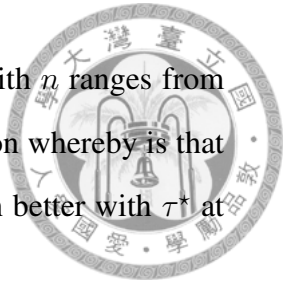

Then, two subfigures as in Fig. 4.4 are generated from Fig. 4.3 with n ranges from $[0, 100]$ to observe practical scenarios more clearly. Another observation whereby is that when $W_0 = 1$, line of τ will have a flat start, which happens to match better with $\tau^\star$ at $n \leq M$.

All above observations are summed up that W_0 has significant influence on scenario of $n \leq M$, while W_m counts when n is large, namely the dense scenario. In the next two subsections, the system efficiency and access delay under different parameter configurations are practically evaluated, whereby above observed effects of parameters could be conformed.

Configure OCW_{max}

With above rough rules, the effect of OCW_{max} is first evaluated by setting different OCW_{max} while fixing $OCW_{min} = 1$ and $M = 9$. In Fig. 4.5a, three lines which have the same OCW_{min} are selected to clearly display the effect of OCW_{max} on system efficiency. From the figure, it is evident that larger OCW_{max} is much better for system efficiency when $n \geq M$. The result corresponds to the above rules obtained from the effect of parameters on τ. The same result is also observed from Fig. 4.5b, where larger OCW_{max} has shorter access delay.

Configure OCW_{min}

To estimate the effect of OCW_{min}, the performance of different configurations of OCW_{min} while fixing large $OCW_{max} = 1023$, and $M = 18$. First, OCW_{min} determines the start of the probability τ, and it has a significant influence on the scenario of $n \leq M$. From Fig. 4.6a and 4.6b, we find the larger $OCW_{min} = 127$ has lower system efficiency and larger access delay. Secondly, as stated in Section 4.2.2 that $W_0 = W_m \leq M$ is the perfect configuration in the scenario of $n \leq M$, it is validated in Fig. 4.6 that maximum system efficiency and minimum access delay are achieved with the configuration in the scenario of $n \leq M$. However, the configuration of small OCW_{min} and large OCW_{max} almost achieves as good performance as the perfect configuration.

doi:10.6342/NTU201700509

4.2.3 Rules for configuring $\{M, OCW_{min}, OCW_{max}\}$

Above two previous subsections, we could conclude rules of configuring the parameter set $\{M, OCW_{min}, OCW_{max}\}$ for obtaining best performance for all n.

1 For M: the larger the better

2 For OCW_{min}, OCW_{max}:

- OCW_{min} counts when $n \leq M$. Smaller OCW_{min} is better.
- OCW_{max} counts when $n > M$. Larger OCW_{max} is better.

- Special case: for $n \leq M$

  $OCW_{max} = OCW_{min} < M$ is the optimal configuration.

doi:10.6342/NTU201700509

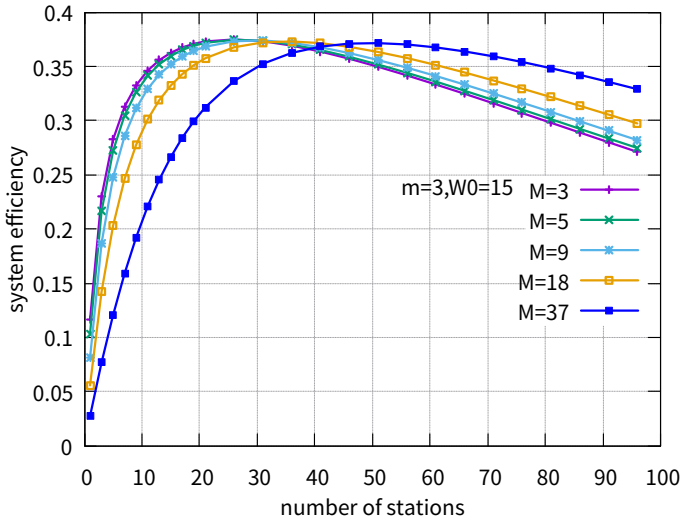

(a) System efficiency versus number of stations

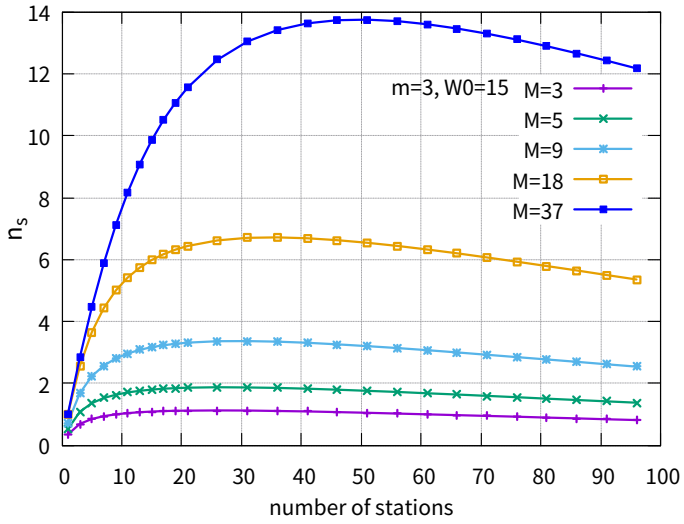

(b) Number of successful stations in a single stage versus number of stations

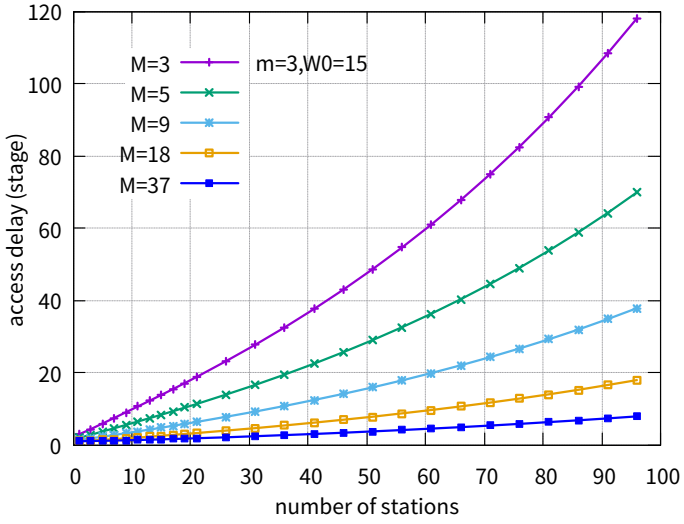

(c) Access delay versus number of stations

Figure 4.2: Configure M

doi:10.6342/NTU201700509

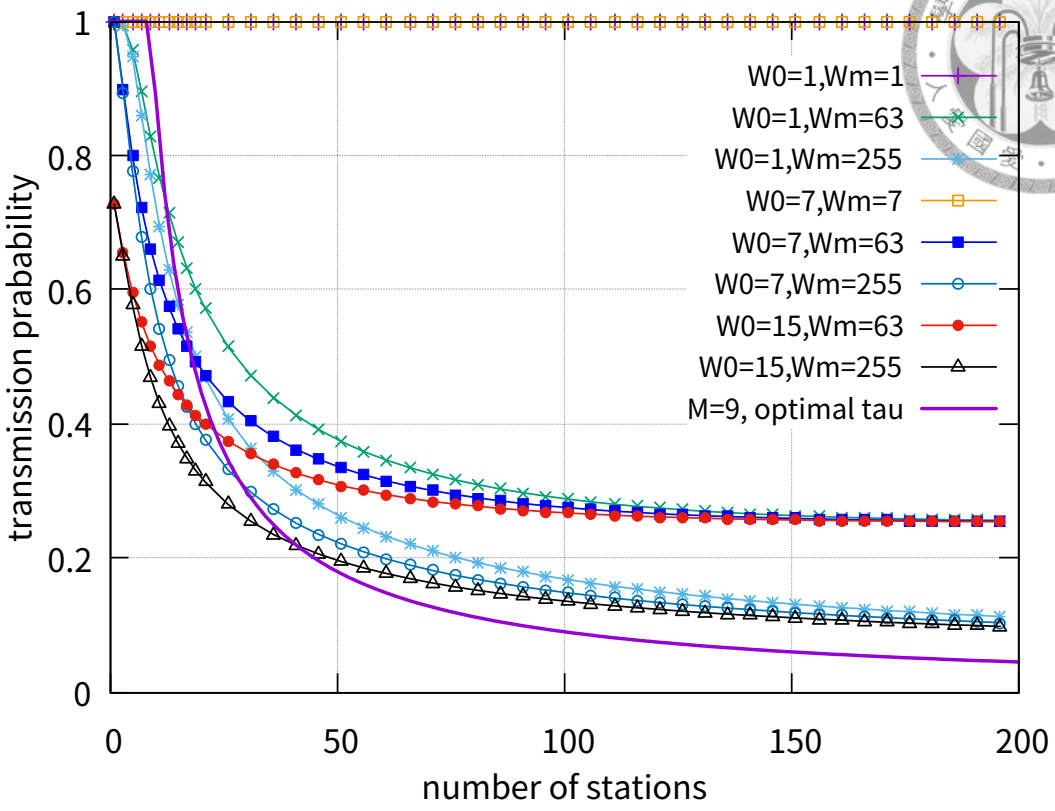

(a) Case 1, given $M = 9$

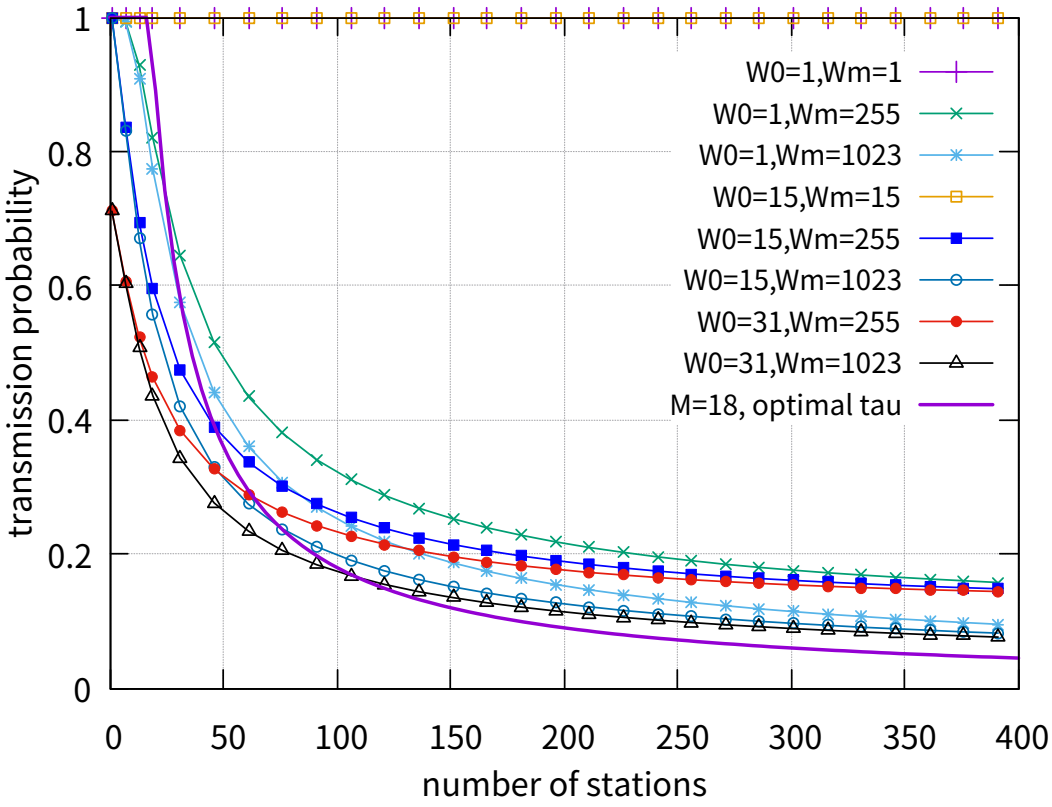

(b) Case 2, given $M = 18$

Figure 4.3: Transmission probability τ versus number of stations

doi:10.6342/NTU201700509

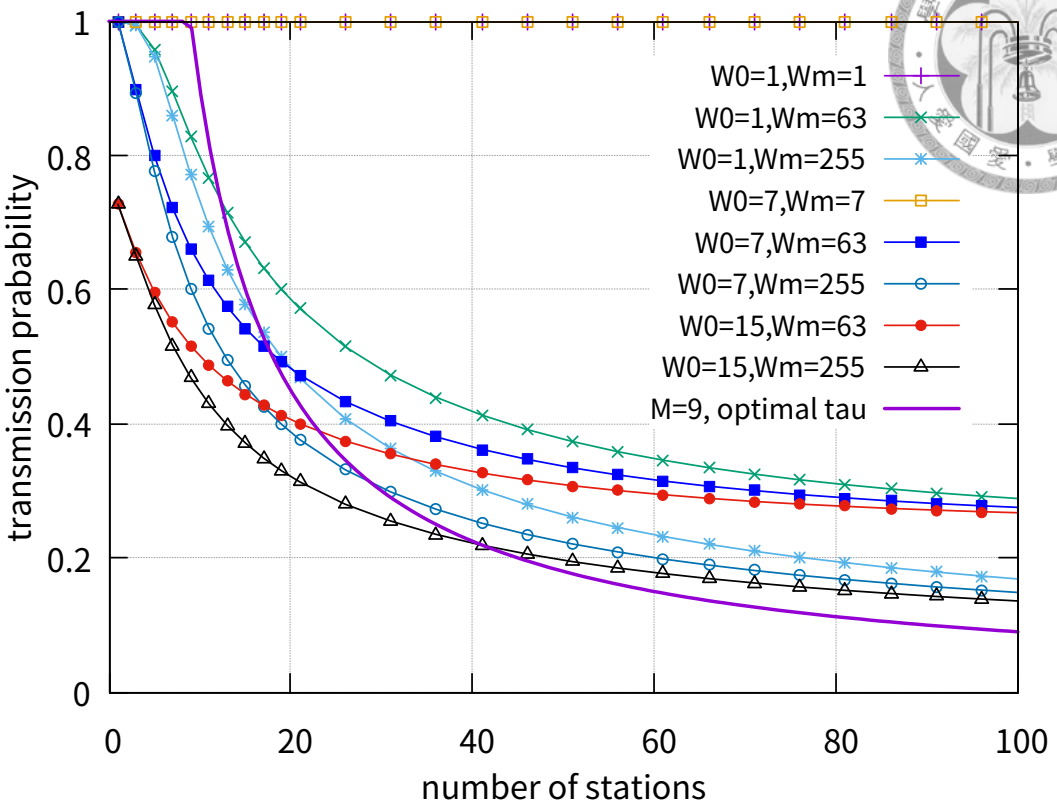

(a) Case 1, given $M = 9$

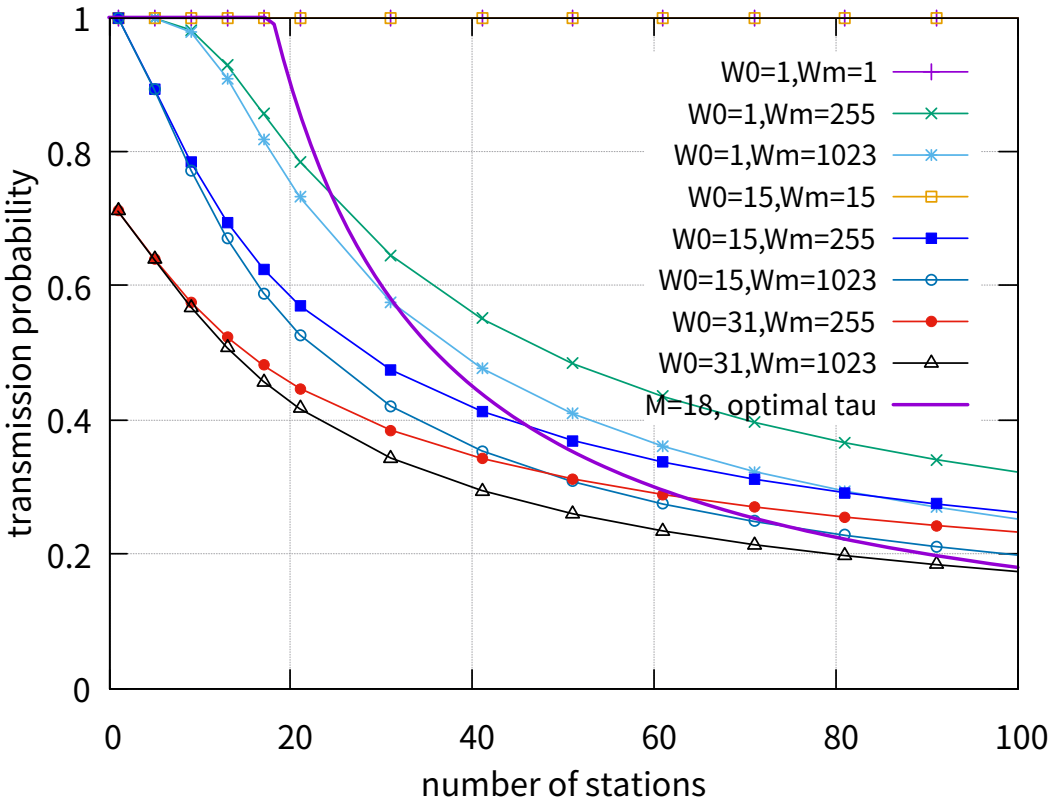

(b) Case 2, given $M = 18$

Figure 4.4: Details of transmission probability τ versus number of stations when $n \leq 100$

doi:10.6342/NTU201700509

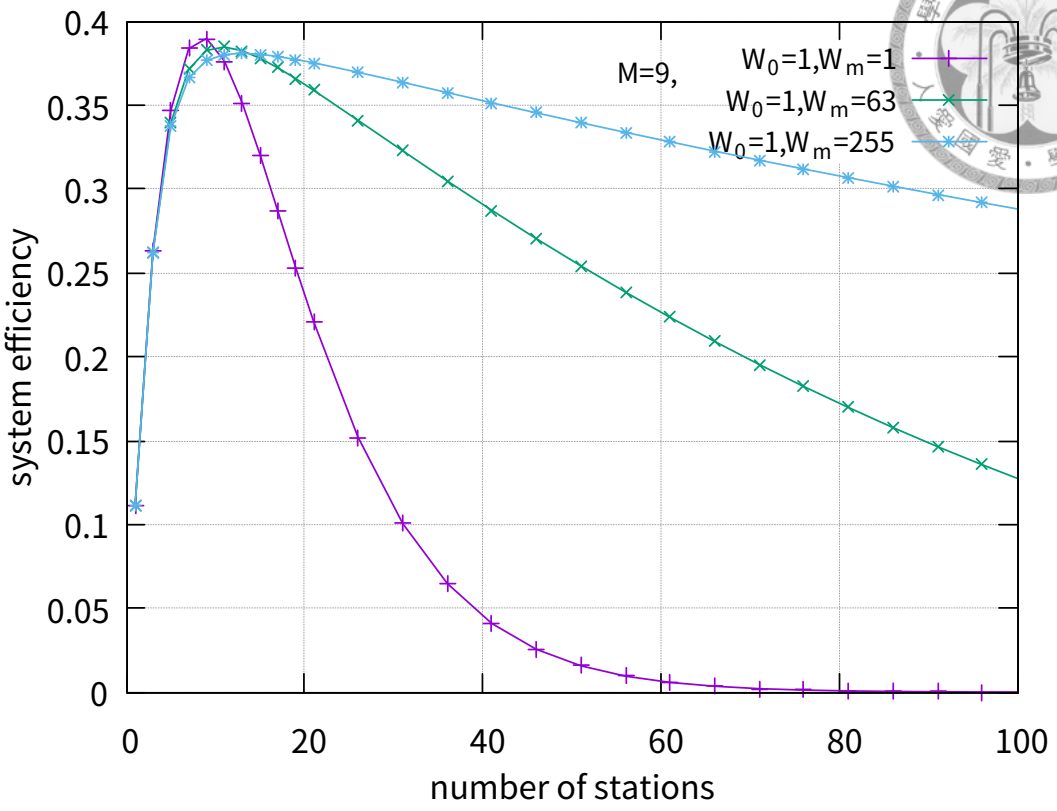

(a) System efficiency versus number of stations

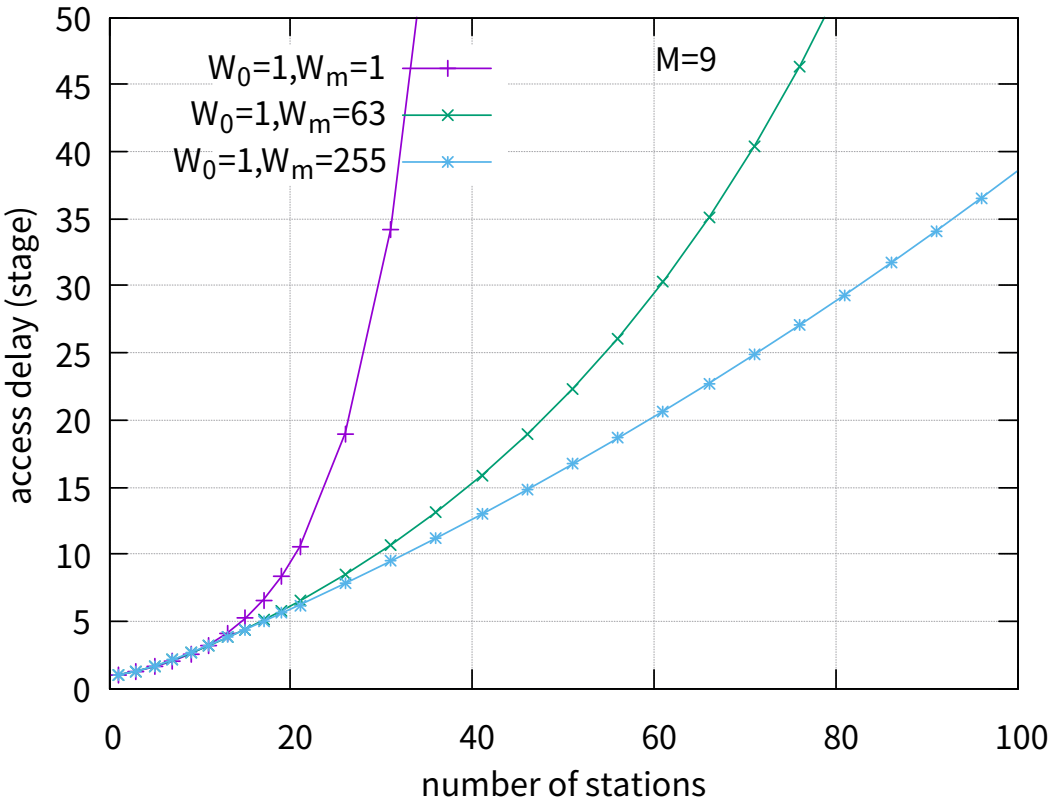

(b) Access delay versus number of stations

Figure 4.5: Example of Configuring OCW_{max}, given $M = 9$

doi:10.6342/NTU201700509

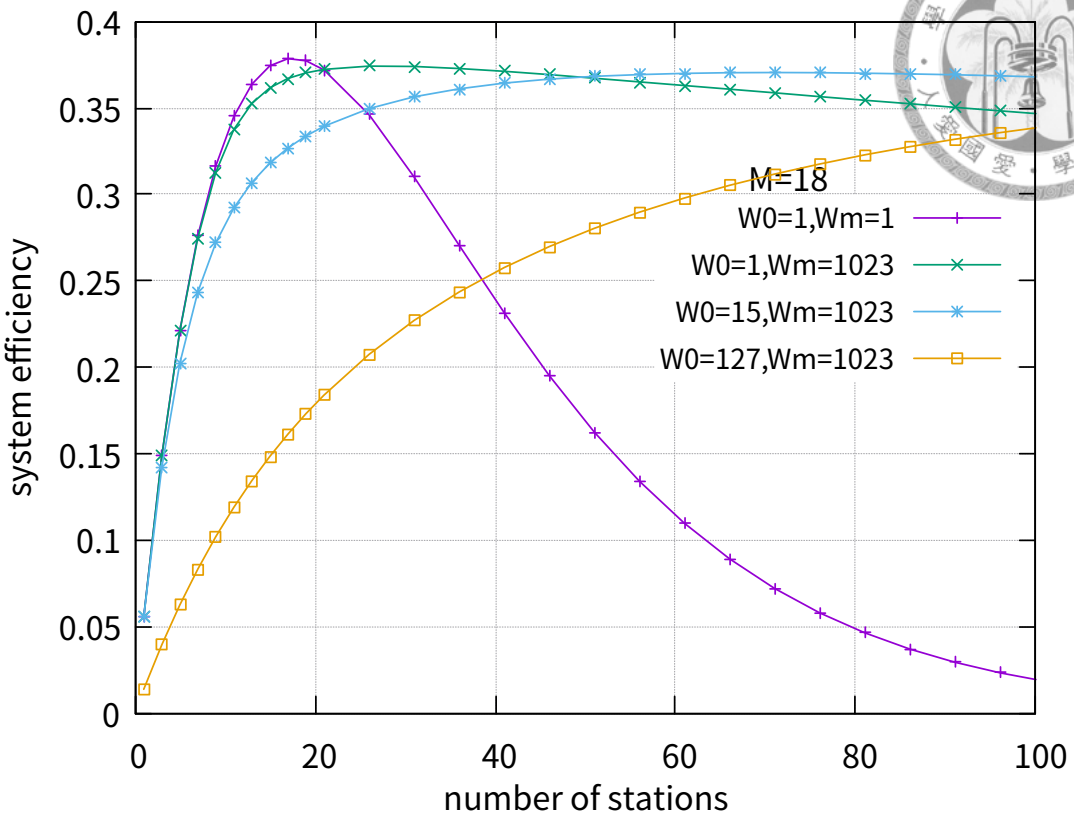

(a) System efficiency versus number of stations

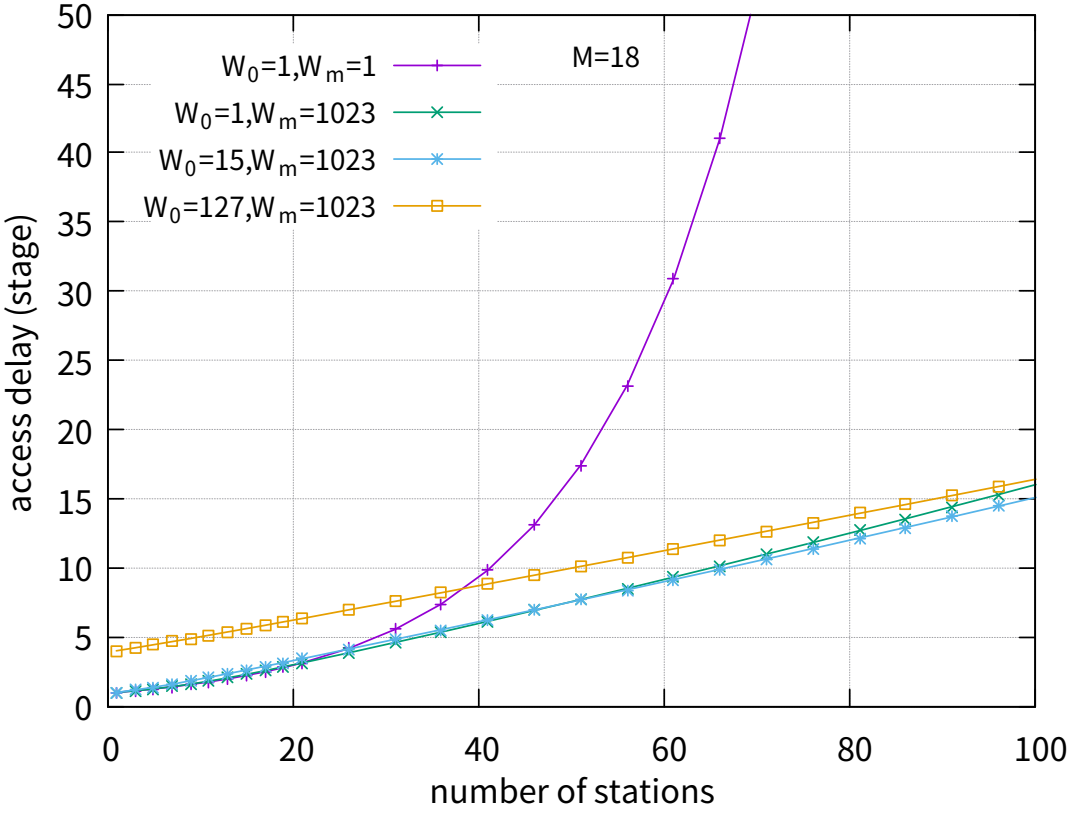

(b) Access delay versus number of stations

Figure 4.6: Example of Configuring OCW_{min}, given $M = 18$

doi:10.6342/NTU201700509

Chapter 5

Conclusion and Future work

In this thesis, we are the first to propose a bi-dimensional Markov chain model conducting saturation analysis of the OBRA of 802.11ax. The Markov chain model is validated that it could accurately depict the steady state behavior of the OBRA. Thereby, closed-form expressions of system efficiency and access delay are derived. Finally, it is observed that performance strongly depends on the system parameters. Larger number of RUs or subchannels for random access results in more successful contending stations in a stage. The initial contention window has significant influence when only a few stations exist, while maximum contention window counts in the dense scenario.

Different from DCF of legacy 802.11, the OBRA mechanism is more flexible, with system parameters dynamically configured. A real-time algorithm is required to configure the system parameters dynamically. This thesis takes the first step to catch some insight from the steady state behavior of the OBRA mechanism. In the future, transient analysis is necessary to generate a configuration algorithm.

doi:10.6342/NTU201700509

Bibliography

[1] "Draft 1.0, Part 11: Wireless LAN Medium Access Control (MAC) and Physical Layer (PHY) Specifications, Amendment 6: Enhancements for High Efficiency WLAN," *IEEE Std. 802.11ax*, pp. 1–376, Dec 2016.

[2] "wikipedia, Open Systems Interconnection model (OSI model)," https://en.wikipedia.org/wiki/OSI_model, [Online; accessed on 10-Dec-2016].

[3] "IEEE 802.11-2012: Wireless LAN Medium Access Control MAC and Physical Layer PHY Specifications," *IEEE 802.11 LAN Standards*, 2012.

[4] "WiFi Alliance," http://www.wi-fi.org/.

[5] H. Lipfert, "MIMO OFDM Space Time Coding–Spatial Multiplexing, Increasing Performance and Spectral Efficiency in Wireless Systems, Part I Technical Basis (Technical report)," *Institut für Rundfunktechnik*, 2007.

[6] O. Bejarano, E. W. Knightly, and M. Park, "IEEE 802.11 ac: from channelization to multi-user MIMO." *IEEE Communications Magazine*, vol. 51, no. 10, pp. 84–90, 2013.

[7] "IEEE std 802.11ac:-2013 Wireless LAN Medium Access Control MAC and Physical Layer PHY Specifications," *IEEE 802.11 LAN Standards*, 2013.

[8] E. Perahia and R. Stacey, *Next Generation Wireless LANS: 802.11 n and 802.11 ac*. Cambridge university press, 2013.

[9] Cisco, "Cisco Visual Networking Index:Forecast and Methodology, 2015-2020," http://www.cisco.com/c/en/us/solutions/collateral/service-provider/

doi:10.6342/NTU201700509

visual-networking-index-vni/complete-white-paper-c11-481360.pdf, [Online; accessed on 13-June-2016].

[10] H. S. Simone Merlin, Gwen Barriac, "TGax Simulation Scenarios," http://www.ieee802.org/11/Reports/tgax_update.htm, July 2015, [Online; accessed on 5-Dec-2016].

[11] S. Baraković and L. Skorin-Kapov, "Survey and challenges of QoE management issues in wireless networks," *Journal of Computer Networks and Communications*, vol. 2013, 2013.

[12] F. Tobagi and L. Kleinrock, "Packet switching in radio channels: Part ii–the hidden terminal problem in carrier sense multiple-access and the busy-tone solution," *IEEE Transactions on communications*, vol. 23, no. 12, pp. 1417–1433, 1975.

[13] D. P. Bertsekas, R. G. Gallager, and P. Humblet, *Data networks*. Prentice-Hall International New Jersey, 1992, vol. 2.

[14] G. Bianchi, "Performance analysis of the IEEE 802.11 distributed coordination function," *IEEE Journal on selected areas in communications*, vol. 18, no. 3, pp. 535–547, 2000.

[15] A. Demers, S. Keshav, and S. Shenker, "Analysis and simulation of a fair queueing algorithm," in *ACM SIGCOMM Computer Communication Review*, vol. 19, no. 4. ACM, 1989, pp. 1–12.

[16] O. Aboul-Magd, "802.11 HEW SG Proposed PAR," http://www.ieee802.org/11/Reports/tgax_update.htm, March 2014, [Online; accessed 5-Dec-2016].

[17] M. Morelli, C.-C. J. Kuo, and M.-O. Pun, "Synchronization techniques for orthogonal frequency division multiple access (ofdma): A tutorial review," *Proceedings of the IEEE*, vol. 95, no. 7, pp. 1394–1427, 2007.

doi:10.6342/NTU201700509

[18] N. Abramson, "THE ALOHA SYSTEM: another alternative for computer communications," in *Proceedings of the November 17-19, 1970, fall joint computer conference*. ACM, 1970, pp. 281–285.

[19] L. G. Roberts, "ALOHA packet system with and without slots and capture," *ACM SIGCOMM Computer Communication Review*, vol. 5, no. 2, pp. 28–42, 1975.

[20] L. Kleinrock and F. Tobagi, "Packet switching in radio channels: Part I-carrier sense multiple-access modes and their throughput-delay characteristics," *IEEE transactions on Communications*, vol. 23, no. 12, pp. 1400–1416, 1975.

[21] K.-C. Chen, "Medium access control of wireless LANs for mobile computing," *IEEE Network*, vol. 8, no. 5, pp. 50–63, 1994.

[22] T.-S. Ho and K.-C. Chen, "Performance analysis of IEEE 802.11 CSMA/CA medium access control protocol," in *proc. PIMRC*, vol. 96, 1996, pp. 407–411.

[23] F. Cali, M. Conti, and E. Gregori, "IEEE 802.11 protocol: design and performance evaluation of an adaptive backoff mechanism," *IEEE journal on selected areas in communications*, vol. 18, no. 9, pp. 1774–1786, 2000.

[24] F. Calì, M. Conti, and E. Gregori, "Dynamic tuning of the IEEE 802.11 protocol to achieve a theoretical throughput limit," *IEEE/ACM Transactions on Networking (ToN)*, vol. 8, no. 6, pp. 785–799, 2000.

[25] Y. S. Liaw, A. Dadej, and A. Jayasuriya, "Performance analysis of IEEE 802.11 DCF under limited load," pp. 759–763, 2005.

[26] F. Daneshgaran, M. Laddomada, F. Mesiti, and M. Mondin, "Unsaturated throughput analysis of IEEE 802.11 in presence of non ideal transmission channel and capture effects," *IEEE Transactions on Wireless Communications*, vol. 7, no. 4, pp. 1276–1286, 2008.

doi:10.6342/NTU201700509

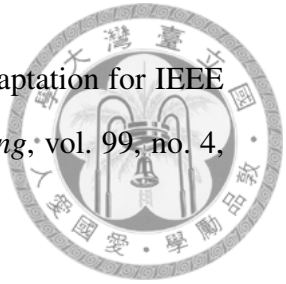

[27] D. Qiao, S. Choi, and K. G. Shin, "Goodput analysis and link adaptation for IEEE 802.11 a wireless LANs," *IEEE transactions on Mobile Computing*, vol. 99, no. 4, pp. 278–292, 2002.

[28] P. Chatzimisios, A. Boucouvalas, and V. Vitsas, "Influence of channel BER on IEEE 802.11 DCF," *Electronics letters*, vol. 39, no. 23, p. 1687, 2003.

[29] Q. Ni, T. Li, T. Turletti, and Y. Xiao, "Saturation throughput analysis of error-prone 802.11 wireless networks," *Wireless Communications and Mobile Computing*, vol. 5, no. 8, pp. 945–956, 2005.

[30] Z.-n. Kong, D. H. Tsang, B. Bensaou, and D. Gao, "Performance analysis of IEEE 802.11 e contention-based channel access," *IEEE Journal on selected areas in communications*, vol. 22, no. 10, pp. 2095–2106, 2004.

[31] I. Rubin, "Group random-access disciplines for multi-access broadcast channels," *IEEE Transactions on Information Theory*, vol. 24, no. 5, pp. 578–592, 1978.

[32] W. Szpankowski, "Packet switching in multiple radio channels: Analysis and stability of a random access system," *Computer Networks (1976)*, vol. 7, no. 1, pp. 17–26, 1983.

[33] M. A. Marsan and M. Bruscagin, "Multichannel Aloha networks with reduced connections," in *IEEE INFOCOM*, vol. 87, 1987, pp. 268–275.

[34] H. Tan and H. Wang, "Performance of multiple parallel slotted Aloha channels," in *Proc. INFOCOM*, vol. 87, 1987, pp. 931–940.

[35] Z. Zhang and Y.-J. Liu, "Multichannel Aloha data networks for personal communications services (PCS)," in *Global Telecommunications Conference, 1992. Conference Record., GLOBECOM'92. Communication for Global Users., IEEE*. IEEE, 1992, pp. 21–25.

doi:10.6342/NTU201700509

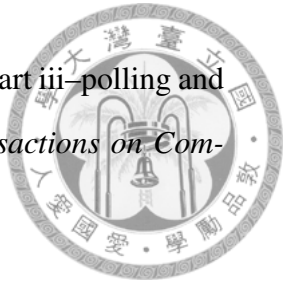

[36] F. Tobagi and L. Kleinrock, "Packet switching in radio channels: Part iii–polling and (dynamic) split-channel reservation multiple access," *IEEE Transactions on Communications*, vol. 24, no. 8, pp. 832–845, 1976.

[37] J. Deng, Y. S. Han, and Z. J. Haas, "Analyzing split channel medium access control schemes," *IEEE Transactions on Wireless Communications*, vol. 5, no. 5, pp. 967–971, 2006.

[38] Y. S. Han, J. Deng, and Z. J. Haas, "Analyzing multi-channel medium access control schemes with aloha reservation," *IEEE Transactions on Wireless Communications*, vol. 5, no. 8, pp. 2143–2152, 2006.

[39] H. Kwon, H. Seo, S. Kim, and B. G. Lee, "Generalized CSMA/CA for OFDMA systems: protocol design, throughput analysis, and implementation issues," *IEEE Transactions on Wireless Communications*, vol. 8, no. 8, pp. 4176–4187, August 2009.

[40] D. Shen and V. O. Li, "Performance analysis for a stabilized multi-channel slotted ALOHA algorithm," in *Personal, Indoor and Mobile Radio Communications, 2003. PIMRC 2003. 14th IEEE Proceedings on*, vol. 1. IEEE, 2003, pp. 249–253.

[41] P. Zhou, H. Hu, H. Wang, and H.-h. Chen, "An efficient random access scheme for OFDMA systems with implicit message transmission," *IEEE transactions on wireless communications*, vol. 7, no. 7, pp. 2790–2797, 2008.

[42] Y.-J. Choi, S. Park, and S. Bahk, "Multichannel random access in OFDMA wireless networks," *IEEE Journal on Selected Areas in Communications*, vol. 24, no. 3, pp. 603–613, 2006.

[43] S. Kim, J. Cha, S. Jung, C. Yoon, and K. Lim, "Performance evaluation of random access for M2M communication on IEEE 802.16 network," in *Advanced Communication Technology (ICACT), 2012 14th International Conference on*. IEEE, 2012, pp. 278–283.

doi:10.6342/NTU201700509

[44] J.-B. Seo and V. C. Leung, "Design and analysis of backoff algorithms for random access channels in UMTS-LTE and IEEE 802.16 systems," *IEEE Transactions on Vehicular Technology*, vol. 60, no. 8, pp. 3975–3989, 2011.

[45] C.-H. Wei, R.-G. Cheng, and S.-L. Tsao, "Modeling and estimation of one-shot random access for finite-user multichannel slotted ALOHA systems," *IEEE Communications Letters*, vol. 16, no. 8, pp. 1196–1199, 2012.

[46] C.-H. Wei, G. Bianchi, and R.-G. Cheng, "Modeling and analysis of random access channels with bursty arrivals in OFDMA wireless networks," *IEEE Transactions on Wireless Communications*, vol. 14, no. 4, pp. 1940–1953, 2015.

[47] D.-J. Deng, S.-Y. Lien, J. Lee, and K.-C. Chen, "On Quality-of-Service Provisioning in IEEE 802.11 ax WLANs," *IEEE Access*.

[48] E. Khorov, A. Lyakhov, A. Krotov, and A. Guschin, "A survey on IEEE 802.11 ah: An enabling networking technology for smart cities," *Computer Communications*, vol. 58, pp. 53–69, 2015.

doi:10.6342/NTU201700509